Changes in chlorophyll concentration and phenology in the North Sea in relation to de-eutrophication and sea surface warming

Xavier Desmit [1]*, Anja Nohe,[2] Alberto Vieira Borges [3], Theo Prins,[4] Karien De Cauwer,[1] Ruth Lagring,[1] Dimitry Van der Zande,[1] Koen Sabbe[2]

[1]Royal Belgian Institute of Natural Sciences, Operational Directorate Natural Environment, Brussels, Belgium
[2]Department of Biology, Protistology & Aquatic Ecology Lab, Ghent University, Ghent, Belgium
[3]Chemical Oceanography Unit, University of Liège, Liège, Belgium
[4]Deltares, Department of Marine and Coastal Systems, Delft, The Netherlands

Abstract

At least two major drivers of phytoplankton production have changed in recent decades in the North Sea: sea surface temperature (SST) has increased by ~ 1.6°C between 1988 and 2014, and the nitrogen and phosphorus loads from surrounding rivers have decreased from the mid-1980s onward, following reduction policies. Long time series spanning four decades (1975–2015) of nutrients, chlorophyll (Chl), and pH measurements in the Southern and Central North Sea were analyzed to assess the impact of both the warming and the de-eutrophication trends on Chl. The de-eutrophication process, detectable in the reduction of nutrient river loads to the sea, caused a decrease of nutrient concentrations in coastal waters under riverine influence. A decline in annual mean Chl was observed at 11 out of 18 sampling sites (coastal and offshore) in the period 1988–2016. Also, a shift in Chl phenology was observed around 2000, with spring bloom formation occurring earlier in the year. A long time series of pH in the Southern North Sea showed an increase until the mid-1980s followed by a rapid decrease, suggesting changes in phytoplankton production that would support the observed changes in Chl. Linear correlations, however, did not reveal significant relationships between Chl variability and winter nutrients or SST at the sampling sites. We propose that the observed changes in Chl (annual or seasonal) around 2000 are a response of phytoplankton dynamics to multiple stressors, directly or indirectly influenced by de-eutrophication and climate warming.

At least two major trends are currently affecting phytoplankton dynamics in the North Sea: the warming trend that started between 1982 and 1987 (Beaugrand and Reid 2003; Edwards et al. 2006; van Aken 2010; Høyer and Karagali 2016) and the de-eutrophication trend, that is, the decreasing loads of nutrients and organic matter into coastal seas, that started in the 1980s (van Beusekom et al. 2009; Burson et al. 2016; Meyer et al. 2018). In addition to potentially altering the stratification regime in the Central North Sea, increasing sea surface temperature (SST) may have strong effects on the physiology of marine phytoplankton, that is, temperature may enhance phytoplankton cell division rate (Hunter-Cevera et al. 2016) or, on the contrary,

negatively affect net production when it exceeds temperature optima for photosynthesis while still enhancing cell respiration (Barton et al. 2018). Richardson and Schoeman (2004) have shown a consistent correlation between the temperature increase and the change in phytoplankton abundance (based on Continuous Plankton Recorder [CPR] counts) in the Northeast Atlantic. They show a decreasing abundance of phytoplankton as SST increases in warmer waters and an increasing abundance of phytoplankton as SST increases in cooler waters, with a northward shift of species. Such temperature effects can then propagate in the food web through bottom-up control of herbivorous copepods by their phytoplankton prey and of carnivorous zooplankton by their copepod prey (Beaugrand and Reid 2003; Richardson and Schoeman 2004; Richardson 2008; Capuzzo et al. 2018). Recently, Capuzzo et al. (2018) showed a correlation between the increase in SST and a decrease in phytoplankton production in the North Sea, with a negative impact on small copepods and fish recruitment. Temperature may also have an effect on the phenology of phytoplankton blooms. Hunter-Cevera et al. (2016) showed how increasing SST in New England coastal waters accelerated phytoplankton cell division rates,

Additional Supporting Information may be found in the online version of this article.

inducing changes in the timing and amplitude of the blooms. This supports the idea that "in a warming climate spring processes tend to occur earlier and autumn processes shift later" (Atkinson et al. 2015). Such shifts in phenology could lead to uncoupling of trophic interactions (Cushing 1990; Edwards and Richardson 2004).

At the same time, human-induced eutrophication at a global scale has caused deleterious effects in coastal zones (e.g., oxygen minimum zones, Harmful Algal Blooms) with potentially serious consequences for ecosystem functioning, such as, for example, massive animal mortality or partial inhibition of secondary production (Galloway et al. 2004; Daro et al. 2006; Diaz and Rosenberg 2008; Doney 2010; Lancelot et al. 2014). The North Sea is subject to relatively high anthropogenic riverine loads of nitrogen (N) and phosphorus (P) (Lancelot et al. 1987; Jickells 1998; Brion et al. 2006) with an additional significant atmospheric input of nitrogen (Troost et al. 2013): 10% to 30% of the nitrogen in the Southern North Sea originates from the atmosphere (Dulière et al. 2017). This drives intense phytoplankton blooms with large phytoplankton biomass accumulation (usually expressed as chlorophyll [Chl]) in most coastal zones between March and October (Cadée and Hegeman 2002; Rousseau et al. 2006; Desmit et al. 2015, 2018; OSPAR_Commission 2017). Depending on the morphology and hydrology of the receiving basin and on phytoplankton community structure, eutrophication may lead to different symptoms such as foam events (caused by blooms of the colonial haptophyte Phaeocystis), hypoxia or even dead zones, nutrient imbalances allowing toxic species occurrence, inhibition of zooplankton egg production, and/or changes in community structure (Jickells 1998; Rousseau et al. 2000; Colijn et al. 2002; Daro et al. 2006; Philippart et al. 2007), and these phenomena can be further complicated by climate change (Painting et al. 2013). Mitigating eutrophication in the North Sea requires the reduction of nutrient inputs to the rivers (de Jonge et al. 2002; Billen et al. 2011), preferably by adopting a dual-N,P reduction strategy to avoid pronounced nutrient imbalances (Howarth and Marino 2006; Conley et al. 2009). At the end of the 1960s, an International Symposium was held at Helgoland during which it was recommended to take immediate measures against marine pollution in the North Sea "even before the urgently required formal international conventions are established" (de Jong 2007). To this end, initiatives like the
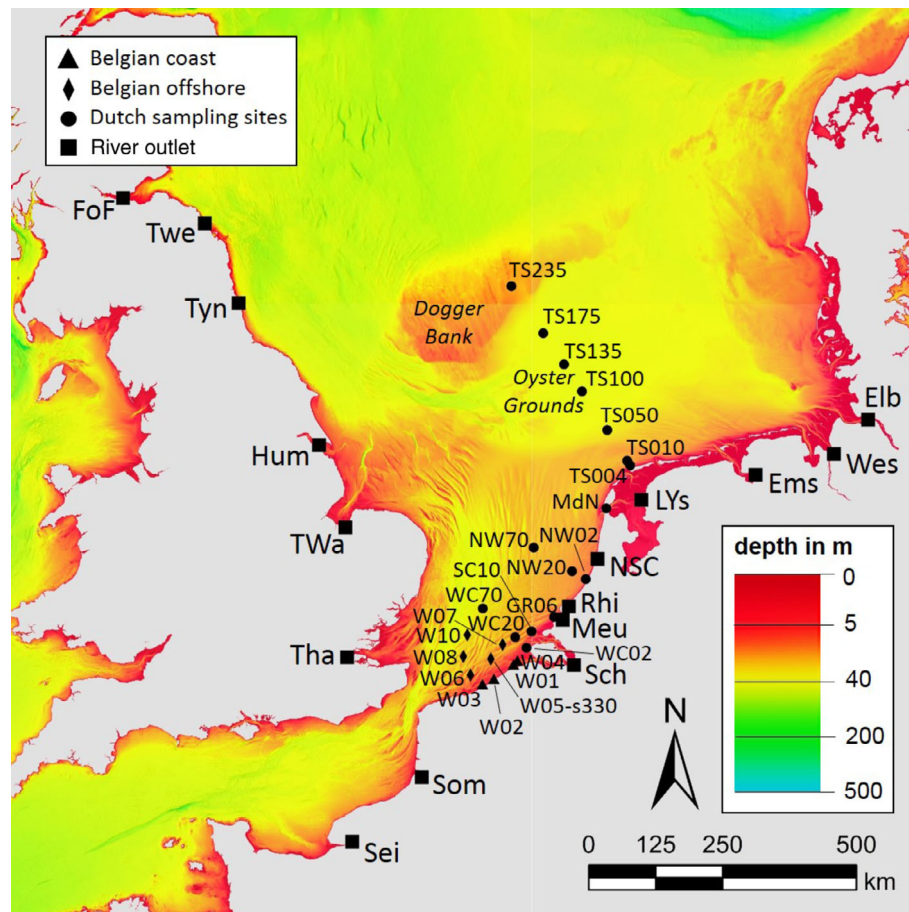
Fig. 1. Bathymetry (source: EMODnet) of the North Sea with the locations of the Belgian and Dutch sampling sites and of the main river outlets (*see* also Tables 1 and 2 for full names of labels). [Color figure can be viewed at wileyonlinelibrary.com]

introduction of secondary treatment in sewage purification plants were taken as early as the 1970s with effects on ammonium and particulate P (van Bennekom and Wetsteijn 1990). Since the late 1980s, countries around the North Sea agreed on measures to reduce nutrient inputs (NSC 1987, 1990). In addition to this agreement at the level of the Regional Sea Convention, European Member States initiated various nutrient reduction policies aiming at the de-eutrophication of rivers and coastal waters, that is, the Water Framework Directive (WFD; Directive 2000/60/EC 2000), focusing on inland ground- and surface waters and including the nearshore coastal waters, and the Marine Strategy Framework Directive (Directive 2008/56/EC 2008) focusing on all marine waters, and more specific policies such as the Urban Waste Water Treatment Directive regulating waste waters (UWWTD; Directive 91/271/EEC 1991), or the Nitrates Directive regulating the use of fertilizers (Directive 91/676/EEC 1991). Since 1990, those measures have resulted in decreases in P and, to a lesser extent, N inputs from several river basins (McQuatters-Gollop et al. 2007; Vermaat et al. 2008; Prins et al. 2012; OSPAR_Commission 2017) and decreasing nutrient concentrations in coastal waters in parts of the Southern North Sea (Philippart et al. 2007; van Beusekom et al. 2009; Prins et al. 2012; OSPAR_Commission 2017).

Both the warming and the de-eutrophication trends may have direct or indirect effects on the long-term annual mean and the phenology of Chl. Methodological limitations make it difficult to capture consistent changes in Chl at the scale of the North Sea: the time series should be long enough to detect trends beyond the annual Chl variability and the study should cover the different hydrodynamic regions which are characterized by different biogeochemical conditions (e.g., Capuzzo et al. 2018). Monitoring changes in phenology, for example, by the characterization of bloom onset (start of the bloom) and timing (day of maximum Chl or abundance), requires long time series with relatively high-frequency sampling (e.g., Mieruch et al. 2010, for phytoplankton species; and Philippart et al. 2010, for Chl *a*). Detecting large-scale regime shifts and subsequent changes in plankton community structure requires time series covering the North Sea over decades (Weijerman et al. 2005; Alvarez-Fernandez et al. 2012). The main aim of the present study is to complement previous studies by reporting long-term changes in SST, nutrient concentrations (N, P), and Chl (phenology and annual mean values) over the last decades at different sampling sites in the Southern and Central North Sea. Our objective is to evaluate if these trends over the past decades can be related to climate warming and/or de-eutrophication.

Table 1. Main river outlets around the North Sea with their geographical location (country and coordinates). The mean discharge and mean loads of total N (Ntot), total P (Ptot), and dissolved silica (DSi) are calculated over the period available in the data set. Ntot in U.K. rivers is approximated by winter DIN. Data made available by Sonja van Leeuwen (NIOZ) and Hermann Lenhart (UHAM), *see* Pätsch et al. (2016). Note that the discharges at "North Sea Canal" and "Lake IJssel" are also Rhine River water which is diverted to the north through the river IJssel and then Lake IJssel. "Meuse" in the table is the discharge point at Haringvliet, which is also partly Rhine River water mixed with water from the Meuse River (Haringvliet is approximately 50% Rhine).

Country	River name	Abbrev.	River group	Lat (°N)	Lon (°E)	Mean discharge (m³ s⁻¹)	Ntot mean load (ton day⁻¹)	Ptot mean load (ton day⁻¹)	DSi mean load (ton day⁻¹)	Period
FR	Seine	Sei	Channel FR	49.480	0.486	479.3	339.1	22.3	145.0	1975–2016
FR	Somme	Som	Channel FR	50.180	1.653	35.6	16.0	0.60	9.5	1975–2016
BE	Scheldt	Sch	Delta	51.370	4.208	132.8	76.3	7.12	46.5	1977–2017
NL	Meuse	Meu	Delta	51.840	4.017	721.5	279.4	14.2	58.1	1977–2017
NL	Rhine	Rhi	Delta	51.980	4.120	1420.6	510.1	37.5	153.6	1977–2017
NL	North Sea Canal	NSC	Frisian coast	52.470	4.600	90.8	31.1	3.1	19.3	1977–2017
NL	Lake IJssel	LYs	Frisian coast	53.070	5.336	507.1	164.6	7.8	62.5	1977–2017
U.K.	Thames (Thames, Medway)	Tha	U.K. South East	51.450	0.402	106.9	148.8	8.1	42.1	1975–2016
U.K.	The Wash (Great Ouse, Nene, Witham)	TWa	U.K. Mid East	52.790	0.369	108.7	232.2	3.8	31.8	1975–2016
U.K.	Humber	Hum	U.K. Mid East	53.620	−0.071	322.9	360.3	19.8	89.5	1975–2016
U.K.	Tyne	Tyn	U.K. North East	55.010	−1.422	58.2	11.0	0.5	7.6	1975–2016
U.K.	Tweed	Twe	U.K. North East	55.770	−1.991	97.1	34.4	0.8	18.8	1975–2016
U.K.	Firth of Forth	FoF	U.K. North East	56.010	−3.361	100.8	13.6	0.9	16.6	1975–2016
GE	Ems	Ems	German bight	53.320	7.254	82.0	49.1	1.6	70.0	1980–2017
GE	Weser	Wes	German bight	53.530	8.572	322.3	153.8	7.0	218.5	1980–2017
GE	Elbe	Elb	German bight	53.870	9.143	694.9	329.0	14.9	213.7	1980–2017

Methods

Study area and nutrient loads

The study focuses on the North Sea and more specifically on the continuum from the Southern Bight of the North Sea (Belgium) to the Frisian coast (the Netherlands), and then to the Central North Sea at the Oyster Grounds and Dogger Bank (*see* Fig. 1 and Tables 1, 2 for location of main river outlets and sampling sites). The Belgian continental shelf (BCS) is shallow (~ 20–50 m) with its coastal zone being permanently well-mixed due to tidal energy and its offshore zone being subject to intermittent stratification in the northeastern part (Ruddick and Lacroix 2006; van Leeuwen et al. 2015). The coastal area is under freshwater influence, mainly from the Scheldt but also from the Rhine/Meuse rivers (Dulière et al. 2017), while the offshore waters are dominated by oceanic inputs including remnants of the buoyant plumes from the Seine and Somme rivers (Ménesguen et al. 2018). In the BCS, the oceanic and freshwater end-members are well-mixed horizontally and vertically by tidal energy, resulting in a decreasing coastal-offshore gradient in salinity, and nutrient and Chl concentrations (Desmit et al. 2015). In its southern part, coastal waters of the Dutch continental shelf (DCS) are dominated by the Rhine/Meuse Region Of Freshwater Influence (Rhine/Meuse ROFI or Delta ROFI), where intermittent salinity stratification may occur with complex spatial patterns subject to wind influence and upwelling induced by tidal straining (de Boer et al. 2009). The offshore waters show more stable circulation patterns under the influence of Atlantic waters from the English Channel. A tidal front occurs in an arc across the Southern North Sea from Yorkshire in the United Kingdom to the Frisian coast in the Netherlands, separating relatively well-mixed waters in the south from intermittently or seasonally stratified waters in the Central North Sea (Longhurst 2007; van Leeuwen et al. 2015).

From the 1980s onward, the N and P loads of major rivers have been decreasing around the North Sea (Brion et al. 2006; van Beusekom 2018). A data set of river discharges and riverine nutrient loads (Table 1) has been set up by Sonja van Leeuwen (NIOZ) in the framework of the OSPAR Intercorrespondence Group of Eutrophication MOdelling (ICG-EMO) collaboration

Table 2. Marine sampling sites with their geographical location, depth, mean salinity, period of Chl sampling, and total number of Chl samples. Belgian data are from BMDC, available at www.bmdc.be. Dutch data are from DONAR, available at https://waterinfo.rws.nl/#!/nav/index/.

Country	Sampling site	Abbrev.	Km from coast	Lat (°N)	Lon (°E)	Marine region	Depth (m)	Mean salinity	Range of salinity	Period of Chl sampling	Total number of Chl samples
BE	W01 - s700	BE coast	5	51.375	3.188	Belgian coast	13	30.8	26.7–34.9	1988–2014	306
BE	W02 - s130	BE coast	3	51.225	2.858	Belgian coast	8	32.3	21.0–35.4	1988–2014	324
BE	W03 - s120	BE coast	5	51.168	2.667	Belgian coast	8	33.6	30.3–34.8	1988–2014	277
BE	W04	BE coast	7	51.418	3.253	Belgian coast	12	31.6	29.3–33.7	2007–2014	26
BE	W05 - s330	BE offshore	25	51.432	2.810	Belgian offshore	21	33.6	30.9–35.5	1988–2014	620
BE	W06 - s315	BE offshore	22	51.263	2.468	Belgian offshore	25	34.3	31.2–35.3	1988–2014	152
BE	W07 - s435	BE offshore	32	51.583	3.008	Belgian offshore	22	34.0	31.9–35.2	1988–2014	149
BE	W08 - s421	BE offshore	45	51.458	2.350	Belgian offshore	21	34.7	31.8–35.6	1988–2014	162
BE	W10	BE offshore	64	51.683	2.417	Belgian offshore	38	34.9	33.9–35.3	2008–2014	24
NL	Walcheren 02	WC02	2	51.549	3.411	Delta ROFI	8	32.0	29.2–34.0	1975–2016	494
NL	Walcheren 20	WC20	20	51.659	3.221	Delta ROFI	22	33.3	30.9–35.1	1975–2016	491
NL	Walcheren 70	WC70	70	51.957	2.679	Delta offshore	30	35.0	34.2–35.5	1977–2016	458
NL	Goeree 06	GR06	6	51.870	3.874	Delta ROFI	9	30.5	22.6–33.4	1975–2016	672
NL	Noordwijk 02	NW02	2	52.261	4.406	Delta ROFI	13	28.9	21.5–32.1	1975–2016	997
NL	Noordwijk 10	NW10	10	52.302	4.302	Delta ROFI	18	30.5	22.7–33.7	1975–2016	629
NL	Noordwijk 20	NW20	20	52.342	4.175	Delta ROFI	20	31.9	27.9–34.2	1975–2016	631
NL	Noordwijk 70	NW70	70	52.583	3.531	Delta offshore	28	34.9	32.8–35.6	1975–2016	566
NL	Marsdiep noord	MdN	-	52.983	4.750	Wadden Sea	16	28.0	6.4–36.0	1976–2016	633
NL	Terschelling 004	TS004	4	53.415	5.151	Delta ROFI	13	32.1	27.8–35.0	1975–2006	405
NL	Terschelling 010	TS010	10	53.461	5.101	Delta ROFI	24	32.7	29.1–35.1	1975–2016	568
NL	Terschelling 050	TS050	50	53.768	4.767	North Sea Front	30	34.3	31.4–35.5	1975–2016	383
NL	Terschelling 100	TS100	100	54.149	4.342	Oyster Grounds	49	34.6	32.3–34.9	1988–2016	372
NL	Terschelling 135	TS135	135	54.416	4.041	Oyster Grounds	35	34.7	33.9–35.0	1988–2016	373
NL	Terschelling 175	TS175	175	54.719	3.692	Oyster Grounds	35	34.7	34.0–35.1	1988–2016	315
NL	Terschelling 235	TS235	235	55.172	3.158	Dogger Bank	18	34.9	33.9–35.2	1988–2016	317

on the basis of data available from Hamburg University (Pätsch et al. 2016). The decrease in nutrient loads to the sea, characteristic of de-eutrophication, is reflected in the riverine nutrient concentrations measured at the river outlets, with some rivers showing a maximum nutrient concentration in the 1980s (Fig. 2; nutrient loads are the result of nutrient concentrations multiplied by the water discharge). Ntot is not available for U.K. rivers and the winter DIN concentration (January–February) is used as a proxy for annual mean Ntot concentration, which may be an underestimate.

Sampling sites

Eight sampling sites (on eighteen), representative of different waterbodies in the North Sea, were studied in more detail in the Result section: BE coast and BE offshore (both representing an aggregation of sampling sites, *see* Table 2); and six sampling sites from different transects in Dutch waters: NW02, NW70, GR06, TS010, TS135, and TS235 (*see* Table 2). The coastal–offshore subdivision in Belgian waters is based on the Belgian definition of coastal sites used in the WFD (Directive_2000/60/EC 2000). Sampling sites W01, W02, W03, and W04 are not strictly within one nautical mile from the coast but they are considered as coastal waterbodies. The other Belgian sites are considered as offshore in this study. Some sampling sites are subject to riverine inputs of nutrients (e.g., NW02) while others are under the influence of Atlantic water (e.g., NW70). Some are permanently well-mixed (i.e., BE coast and BE offshore), while others are within the Delta ROFI and may be subject to intermittent saline stratification (GR06, NW02, and TS010). Along the Terschelling transect, there is a deeper offshore site at Oyster Grounds (TS135) and a shallower one at Dogger Bank (TS235), both subject to seasonal thermal stratification.

Data set

The Belgian marine data set includes environmental variables (e.g., SST, salinity, nutrients, Chl, and pH) since the
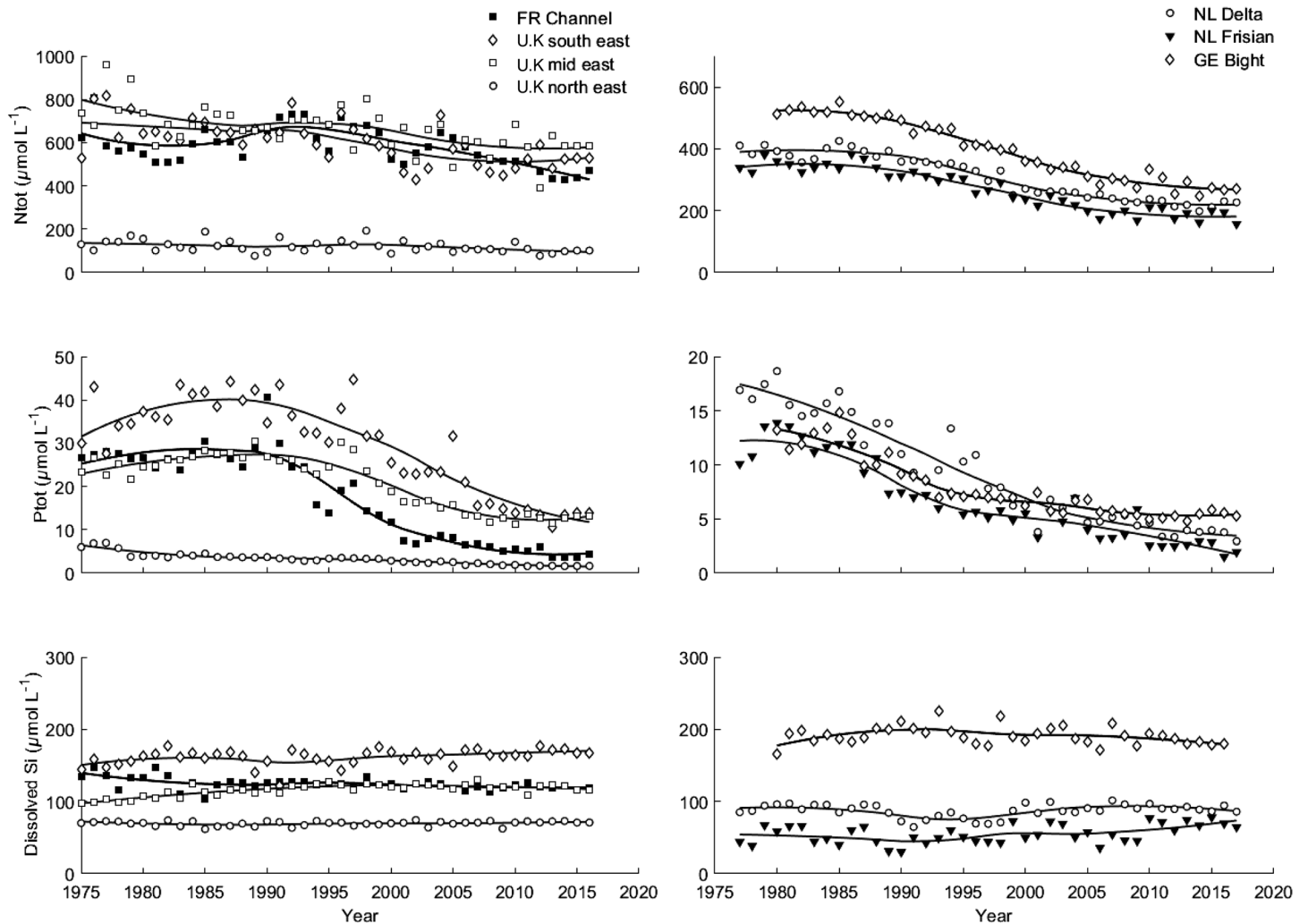
Fig. 2. Annual mean riverine nutrient concentrations (aggregated per region, *see* Table 1). The lines are smooth responses (LOESS, locally estimated scatterplot smoothing; MATLAB 2018) to the annual variability of nutrient concentrations. Ntot in U.K. rivers is approximated by winter DIN.

1970s and documents many different sampling sites in the Southern North Sea (Nohe et al. 2018). The analyzed data set includes nutrients between 1990 and 2014 and Chl between 1988 and 2014. Water samples were taken at the surface of the water column (< 3 m) with a monthly frequency. Gaps in the time series of Chl are frequent in the data set. To reduce their effect, we have aggregated the nine main Belgian sampling sites into two waterbodies: Belgian coast and Belgian offshore (Fig. 1 and Table 2).

Regarding Chl measurements in Belgian waters, several techniques (monochromatic spectrophotometry, fluorimetry, and HPLC) have been used by different laboratories and by different technicians since 1988, possibly introducing random errors of up to 10% in the data (*see* Supplemental Information for details; Table S1).

Salinity and SST were measured in situ with a Seabird SCTD SBE09 or SBE19. Major nutrient concentrations in Belgian waters (ammonium, nitrate, nitrite, and phosphate) were measured using spectrophotometry (for details, *see* Koroleff [1969] for ammonium, De Galan et al. [2004] for nitrate and nitrite, and Van Der Zee and Chou [2005] for phosphate). A Technicon Auto Analyzer II technique was used in the framework of the Belgian monitoring program since 1995 and a Skalar continuous flow system (Auto Analyzer) since 2001. The most important difference lies in the accuracy of the results, with better detection limits and smaller standard deviations (Lagring 2018).

The measurement of pH was done with a glass electrode calibrated with standard buffers in the National Bureau of Standards scale. Initial data analyses showed that there were no difference in trends in the BE coast and BE offshore sites, so data were aggregated to simplify data processing and analysis. In order to detect a possible change in the seasonality of pH (more specifically in the spring), the monthly anomalies of pH in April and May in the BCS have been computed as the monthly average minus the annual average in order to eliminate the long-term trend.

The Dutch marine monitoring program (Rijkswaterstaat 2009) has been measuring environmental variables (e.g., SST, salinity, nutrients, Chl, dissolved oxygen, pH, phytoplankton species composition) on a bi-weekly to monthly basis (depending on the sampling site) since the 1970s along a series of transects perpendicular to the coast, from the Delta region to the Frisian coast (Fig. 1 and Table 2). In this study, we focused on data resulting from subsurface samplings (< 3 m). Dissolved inorganic nitrogen (DIN; detection limit [d.l.] = 0.5 μM) and dissolved inorganic phosphorus (DIP; d.l. = 0.06 μM) were measured following Grasshoff et al. (1983). Chl was determined by fluorescence prior to 1986 and by HPLC from 1986 to today (*see* Supplemental Information Table S1, for details).

We investigated possible changes in the wind climate as wind may influence the duration of the stratification at sea and hence Chl bloom dynamics. As no offshore wind data

were available, we used data from three stations along the Dutch coast (Vlissingen, Hoek van Holland, IJmuiden), obtained from the Dutch meteorological institute (downloaded from www.knmi.nl).

The SST data have been spatially aggregated across all available sampling sites in the North Sea (Belgian and Dutch), yielding the time series called SST_{NS} in this study. A cumulative sum (CuSum) of SST_{NS} was calculated to detect changes in the trend. A CuSum is the sequential sum of the successive elements of a vector having been reduced to zero mean and unit variance (*see* e.g., Beamish et al. 1999). Starting and ending with zero, the CuSum function is typically used for monitoring a change. A positive slope of the CuSum indicates an above-average tendency in the data and a negative slope represents a below-average tendency.

Missing data

Twelve missing data points (out of 528 data points, i.e., 2%) in the monthly SST_{NS} data set have been imputed with a smoothing spline function. Nutrient data sets from rivers were delivered without missing data. Monthly marine nutrient and Chl data showed missing data that have not been replaced and were considered as "not available" (NA). For the purpose of calculating annual mean Chl and the seasonality of Chl time series, years with too few monthly Chl data have been excluded based on the following criteria: a year was excluded if the number of months with no data was > 4
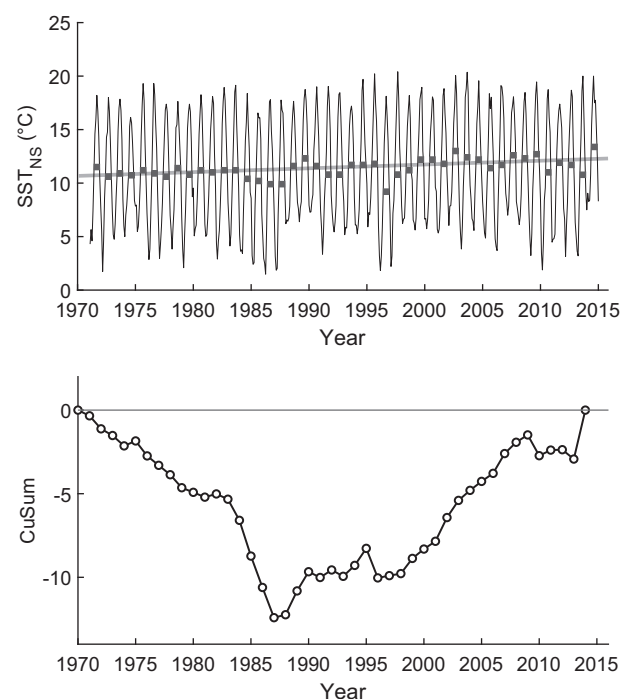
Fig. 3. (Top) Monthly mean (line) and annual mean (squares) SST_{NS}. The gray line is the linear regression on annual mean SST_{NS} (slope = 3.55×10^{-2}; $R^2 = 0.28$; $p = 1.6 \times 10^{-4}$). (Bottom) Cumulative sum of the annual mean SST_{NS} (z-score) in the period 1971–2014.

or if there were no data in the period March to May. For the purpose of nonparametric trend analysis, missing data in annual time series were imputed (see below).

Nonparametric trend test and correlations

The time series of annual winter nutrient concentrations (January–February) and annual mean Chl (whole year) have been submitted to the nonparametric Mann-Kendall's trend test at all sites (*see* equations in Pohlert 2016). Eight representative sampling sites (see above) were selected for the graphics. For the winter nutrients time series, a Pettitt's test (Pettitt 1979) was first applied to detect possible shifts in the central tendency of the time series around a single change-point (a specific year). The Pettitt's test is "true" when two periods show different averages. Then, the Mann–Kendall's trend test was performed on the two periods (or on the whole time series if no change-point was detected). The application

of two trend analyses, that is, before and after the change-point, is particularly indicated in the case of a time series showing different decreasing rates over the period. The null hypothesis in Mann–Kendall's test is that the data are independent and randomly ordered. This test is nonparametric, as it does not rely on any assumptions on the distributions of X or Y. The Kendall rank coefficient (tau) allows establishing whether two variables may be regarded as statistically dependent. Tau varies between −1 (anticorrelation) and 1 (correlation); if X and Y are independent, the coefficient approaches 0. Statistics of significant trends were reported and the parameters of the linear regression were identified with the Sen's test (*see* Pohlert 2016).

For the annual mean Chl data set, the procedure was slightly different: a Mann–Kendall's test was conducted from the year 1988 onward as 1988 is the year of a regime shift in
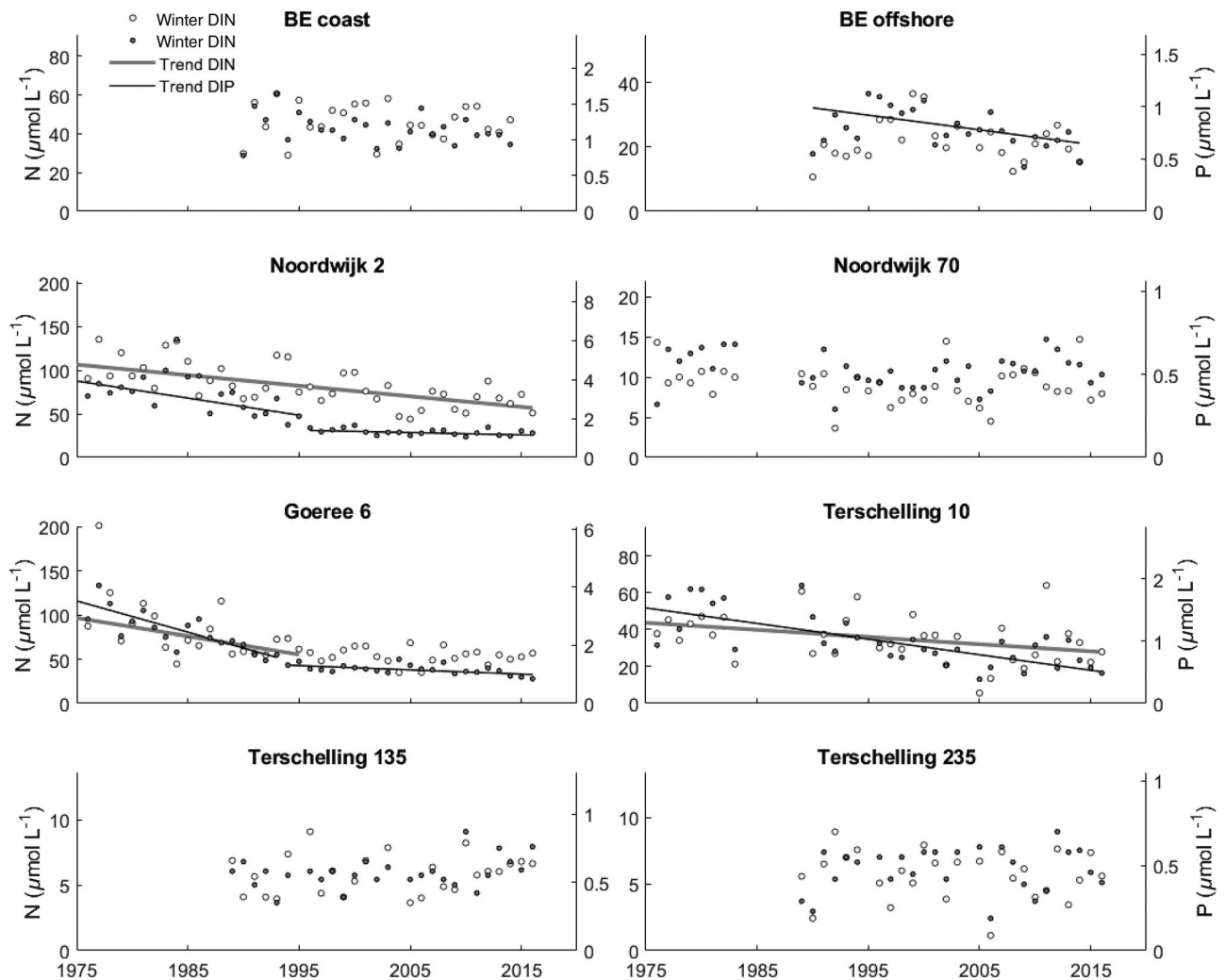
Fig. 4. Annual time series of winter DIN (left axis) and DIP (right axis) concentrations (January–February) for selected sites in the North Sea. The lines show the estimated trend regressions (*see* Table 3) when statistically significant. The waterbodies "BE coast" and "BE offshore" result from the spatial aggregation of the corresponding sampling sites (*see* Table 2).

Table 3. Statistics of trend analyses of the winter nutrient concentration time series for sites where a significant trend was detected (the test was made on the 18 sites). The waterbody "BE offshore" results from the spatial aggregation of the Belgian offshore sampling sites (*see* Table 2).

|	BE offshore N winter	BE offshore P winter	Walcheren 02 N winter	Walcheren 02 P winter	Walcheren 20 N winter	Walcheren 20 P winter	Goeree 06 N winter	Goeree 06 P winter	Noordwijk 02 N winter	Noordwijk 02 P winter	Noordwijk 10 N winter	Noordwijk 10 P winter	Noordwijk 20 N winter	Noordwijk 20 P winter	Marsdiep Noord N winter	Marsdiep Noord P winter	Terschelling 04 N winter	Terschelling 04 P winter	Terschelling 10 N winter	Terschelling 10 P winter	Terschelling 50 N winter	Terschelling 50 P winter
Period of the whole time series	1990–2014		1976–2016		1976–2016		1976–2016		1976–2016		1976–2016		1976–2016		1976–2016		1976–2006		1976–2016		1976–2016	
Mann-Kendall's trend (ci 0.05)	No	Yes	Yes	Yes	Yes	Yes	Yes	Yes	Yes	Yes	Yes	Yes	Yes	Yes	No	Yes	Yes	Yes	Yes	Yes	Yes	Yes
Sen's slope	-	−1.40E-02	−2.64E-01	−2.42E-02	−3.51E-01	−2.15E-02	−9.58E-01	−5.15E-02	−1.21E+00	−7.15E-02	−4.10E-01	−3.87E-02	−4.57E-01	−2.94E-02	-	−5.23E-02	−5.44E-01	−3.67E-02	−3.84E-01	−2.50E-02	−6.63E-02	−2.37E-03
Sen's intercept	-	28.91	574.2	49.73	730.5	44.00	1976	104.5	2506	144.9	873.6	78.68	951.2	59.82	-	105.9	1121	74.40	802.6	50.91	142.1	5.324
Kendall's tau correlation	-	−0.297	−0.246	−0.562	−0.338	−0.605	−0.460	−0.771	−0.484	−0.686	−0.237	−0.777	−0.446	−0.692	-	−0.748	−0.370	−0.600	−0.269	−0.539	−0.338	−0.240
p value	-	4.0E-02	2.5E-02	2.5E-07	1.9E-03	3.2E-08	2.4E-05	1.7E-12	8.7E-06	3.1E-10	3.0E-02	9.8E-13	4.1E-05	2.2E-10	-	7.7E-12	3.7E-03	2.7E-06	1.4E-02	8.1E-07	2.1E-03	3.0E-02
Single change-point																						
Pettitt's single change-point	No	No	Yes	Yes	Yes	Yes	Yes	Yes	Yes	Yes	Yes	Yes	Yes	Yes	No	Yes	No	Yes	No	Yes	Yes	Yes
Year of possible shift in central tendency	-	-	1995	1995	1989	1990	1995	1993	2000	1995	2003	1995	1999	1991	-	1994	-	1990	2001	1995	1996	1987
Period 1																						
Mann-Kendall's trend (ci 0.05)	No	No	No	No	No	No	Yes	Yes	No	Yes	No	Yes	No	No	No	Yes	No	No	No	No	No	No
Sen's slope in 1st period	-	-	-	-	-	-	−2.05E+00	−1.08E-01	-	−8.80E-02	-	−5.34E-02	-	-	-	−7.60E-02	-	-	-	-	-	-
Sen's intercept in 1st period	-	-	-	-	-	-	4154	216.5	-	177.7	-	108.0	-	-	-	153.1	-	-	-	-	-	-
Kendall's tau correlation	-	-	-	-	-	-	−0.368	−0.691	-	−0.396	-	−0.484	-	-	-	−0.487	-	-	-	-	-	-
p value	-	-	-	-	-	-	2.5E-02	8.0E-05	-	1.6E-02	-	3.2E-03	-	-	-	4.5E-03	-	-	-	-	-	-
Period 2																						
Mann-Kendall's trend (ci 0.05)	No	No	No	No	No	No	No	Yes	No	Yes	Yes	Yes	No	Yes	No	Yes	No	Yes	No	No	No	No
Sen's slope in 2nd period	-	-	-	-	-	-	-	−1.47E-02	-	−1.19E-02	-	−1.73E-02	-	−1.56E-02	-	−1.68E-02	-	−2.74E-02	-	-	-	-
Sen's intercept in 2nd period	-	-	-	-	-	-	-	30.71	-	25.21	-	35.75	-	32.24	-	34.71	-	55.68	-	-	-	-
Kendall's tau correlation	-	-	-	-	-	-	-	−0.449	-	−0.317	-	−0.593	-	−0.441	-	−0.491	-	−0.441	-	-	-	-
p value	-	-	-	-	-	-	-	3.3E-03	-	4.9E-02	-	2.0E-04	-	2.2E-03	-	1.6E-03	-	2.1E-02	-	-	-	-

the northeast Atlantic ocean, the North Sea, and the Wadden Sea, with a change in the abundance and composition of plankton species (Beaugrand and Reid 2003; Weijerman et al. 2005; Alvarez-Fernandez et al. 2012). A Pettitt's test was also performed on annual time series of Chl to indicate possible change-points but we did not see an added value in breaking the trend before and after the change-point. We simply calculate the mean Chl in the two periods if there is a change-point. The whole package of trend analysis (packages "kendall," boot," and "trend") is freely available in R (R Core Team 2015). Default parameters for all functions were used in our analyses. These packages require continuous time series without missing data. For the purpose of conducting the trend analyses only, the missing data in our time series have been imputed with the R function "na.approx." That function interpolates between existing data and allows capturing a trend with Mann–Kendall's test in spite of missing data, as was tested by Ramos and Cordeiro (2013).

In addition to trend tests, correlations between annual mean Chl and winter DIN, DIP, or annual SST were assessed for all sites. Statistical significance of all correlations is associated to a threshold alpha of 5% (i.e., significance is obtained at p value < 0.05).

Timing and onset of the Chl spring bloom

One of our objectives was to detect whether there is a significant change in Chl phenology over time, more specifically a change in the timing (time of maximum Chl) and onset (starting time) of the spring bloom. The timing and onset of the Chl spring bloom were determined using a method described for a Chl a time series by Philippart et al. (2010) and for a phytoplankton abundance time series by Mieruch et al. (2010), where a smoothing model function is used to represent the bloom. To demonstrate the feasibility of the method, we first focused on a test site (Noordwijk 10) with the highest sampling frequency (biweekly) of the whole data set. For each year, a smoothing spline interpolation function was used to reproduce the seasonal Chl pattern (MATLAB function "fit" with option "smoothingspline" and smoothing parameter $\lambda = 0.05$; MATLAB 2018). Focusing on the first Chl bloom in spring, we identified the timing of the bloom as the maximum value of the spline function before
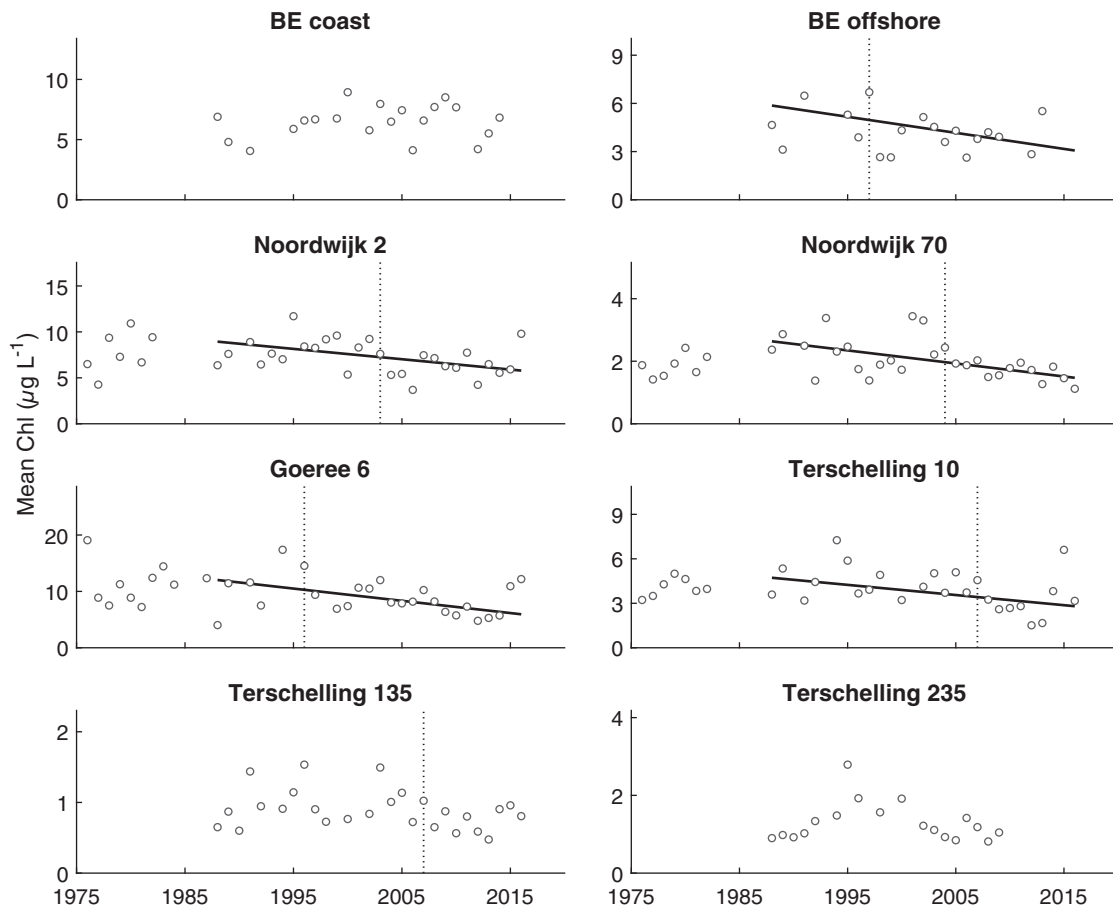
Fig. 5. Time series of annual mean Chl values with their trends (if significant, black lines; see statistics in Table 4) after 1987 for representative sampling sites in the North Sea. The vertical dashed lines indicate the years where a shift in central tendency (Pettitt's test) was detected, if any.

day 150. The instantaneous rate of Chl increase was then estimated on small time intervals (3 days) of the spline curve (local slope of linear regressions, cf. Mieruch et al. 2010) from the beginning of the year to the day of the maximum bloom. Increments of the instantaneous rates were then calculated to determine the acceleration of the Chl bloom increase. The onset of the spring bloom was identified as the day of the maximum acceleration value. As the maximum acceleration was often found close to the Chl maximum, we constrained the search for the onset to periods with Chl values below 25% of the Chl maximum. This algorithm was applied to the annual Chl seasonal profiles at Noordwijk 10 to derive a time series of spring bloom timings and onsets (Fig S1 in Supplemental Information). The same was then applied on climatological years of Chl by decade at Noordwijk 10 (Chl was averaged by decade in 15-day bins; Figs. S1, S2 in Supplemental Information). The subdivision by decade was chosen as an objective slicing of the long time series also reducing the interannual variability. We then used this approach for all other sampling sites to detect the timing and onset of spring bloom for each decade (i.e., avoiding interannual variability and focusing on decadal variability). The smoothing property of the spline function was not used (smoothing parameter $\lambda = 1$) because the monthly averaging already resulted in sufficient smoothing of the Chl seasonal. Linear least-square regressions were then applied for each sampling site separately and also for all sampling sites together to evaluate general tendencies in the timing and onset of the spring bloom. Statistical significance of all regression lines is associated to a threshold alpha of 5% (i.e., $p < 0.05$). Only significant regressions are reported.

Standardization of Chl values in March and May

If changes in Chl spring bloom phenology occur, then the Chl values in March should change from year to year, that is, concentrations would increase over the years in the case of an earlier spring bloom or decrease in the case of a later bloom. Before analyzing such changes, we removed any long-term trends in Chl from the data using the multiplicative model of Cloern and Jassby (2010). Chl in March was thus standardized using the following equation:

$$\text{Chl}^{\text{March}}_{\text{standardized}} = \frac{\text{Chl}^{\text{March}}_y}{A_y} \tag{1}$$

where $\text{Chl}^{\text{March}}_y$ is the monthly value of Chl in March of year y, and A_y is the annual mean Chl of year y. To compare the resulting values of $\text{Chl}^{\text{March}}_{\text{standardized}}$ across sampling sites, the z-scores (vector reduced to zero mean and unit variance) were calculated per sampling site throughout the period 1976–2016. The same approach was also done for Chl in May.

Results

Sea surface temperature and wind

The annual mean SST_{NS} shows an increasing trend over the period 1971–2014 (Fig. 3), corresponding to a temperature increase of 1.6°C, which is consistent with the findings of van

Table 4. Statistics of trend analyses performed on time series of annual mean Chl concentrations at all studied sampling sites in the North Sea (only significant results are presented). The years of possible shifts in the central tendency are indicated with Chl means before and after the shift, and with the relative differences in Chl between periods. The waterbody "BE offshore" results from the spatial aggregation of the Belgian offshore sampling sites (*see* Table 2).

	Statistics of annual mean Chl								
	Period 1988 onward				**Single change-point**				
Sampling site	**Sen's slope**	**Sen's intercept**	**Kendall's tau correlation**	**p value**	**Pettitt's single change-point**	**Year of possible shift in central tendency**	**Mean Chl in period 1**	**Mean Chl in period 2**	**Decrease in Chl between periods**
BE offshore	−1.00E-01	204.7	−0.337	1.7E-02	Yes	1997	5.02	3.85	−23%
WC70	−3.33E-02	68.83	−0.312	2.1E-02	Yes	2004	2.38	1.76	−26%
GR06	−2.17E-01	443.7	−0.277	3.7E-02	Yes	1996	11.2	8.30	−26%
NW02	−1.13E-01	232.6	−0.307	2.4E-02	Yes	2003	8.00	6.24	−22%
NW10	−1.00E-01	205.4	−0.374	5.1E-03	Yes	2002	6.63	4.59	−31%
NW20	−8.33E-02	171.5	−0.310	2.0E-02	Yes	2002	5.90	4.04	−32%
NW70	−4.17E-02	85.47	−0.424	1.6E-03	Yes	2004	2.19	1.67	−24%
MdN	−1.60E-01	328.8	−0.534	5.8E-05	Yes	1995	10.7	7.54	−29%
TS010	−6.85E-02	140.9	−0.296	2.7E-02	Yes	2007	4.47	3.12	−30%
TS050	−1.33E-02	27.89	−0.442	8.9E-04	Yes	1995	1.60	1.18	−26%
TS100	−2.00E-02	41.00	−0.393	3.8E-03	Yes	2003	1.18	0.79	−33%
TS135	-	-	-	-	Yes	2007	0.98	0.74	−25%

Aken (2010) for a selection of Dutch monitoring sites. There are marked differences in annual mean SST_{NS} from one year to the other in 1988 (warmer winter), 1996 (colder winter), and 2014 (warmer winter).

The CuSum of SST_{NS} (Fig. 3, bottom) suggests that there are two tipping points in the increasing trend, that is, 1987–1988 and 1996–1998. While the years 1995–1998 show a negative annual NAO index, we did not find any correlation between the annual means of SST_{NS} and NAO index in the long term. A Pettitt's test made on SST_{NS} shows a shift in the central tendency around the year 1987. The period 1971–1987 has a mean SST_{NS} of 10.6°C while the period 1988–2014 has a mean SST_{NS} of 11.5°C.

There was a significant decrease in the number of days where wind force (hourly averaged wind speed) exceeded 17.1 m s^{-1} (33 knots) during the months March-September in the years 1975–2018 (Mann–Kendall's test, $p < 0.05$).

Nutrients

Figure 4 shows changes in winter DIN and/or DIP (January–February) for eight representative sites in the BCS and DCS (cf. Methods section). Significantly decreasing trends (Mann–Kendall's test) were detected in winter DIN and/or DIP (January–February) at 11 out of 18 sampling sites (Table 3). The decrease in winter DIN (when significant) is continuous over the period except at Goeree 6 where the decrease is significant until 1995 but not afterward. Winter DIP exhibits markedly decreasing concentrations at all sampling sites under freshwater influence, except in BE coast (data only since 1988). In this vertically well-mixed waterbody, neither winter DIN nor DIP concentrations showed a significant trend in the period 1990–2014, in contrast with a decreasing rate of Ntot in the "NL Delta" river group of on average 5.7 μmol L^{-1} year^{-1} during this period (linear regression; $R^2 = 0.88$; $p = 6.8 \times 10^{-20}$). The shallow and well-mixed BE offshore waterbody and site Terschelling 50 are the only offshore areas showing a decreasing trend in winter DIP. The other offshore sampling sites (e.g., Terschelling 135 and 235, Fig. 4) show stable winter nutrient concentrations with relatively low interannual variability.

The Pettitt's test detected a single change-point at 10 sampling sites, namely 8 change-points in winter DIN time series and 10 change-points in winter DIP time series. These change-points occur mainly around the early 1990s, that is, between 1989 and 2003 for winter DIN, and between 1987 and 1995 for winter DIP.

Annual mean Chl

Time series of annual mean Chl values since 1988 show decreasing trends at several sampling sites (Fig. 5 and Table 4). The Mann–Kendall's test identified significant trends at eleven sites in total, all decreasing. Change-points (Pettitt's test) in the central tendency were observed between 1995 and 2007 at twelve sites, with annual means of Chl consistently decreasing by 22% to 33% from one period to the other (Table 4).

The seasonal profile of Chl averaged by decade at eight representative sites suggests a shift in Chl phenology at several sites, with earlier spring bloom formation and termination, especially in the 2000s and 2010s (Fig. 6). Any change in the autumn Chl bloom is less clear, with the exception of Terschelling 10 and Terschelling 235 where the autumn bloom tends to occur later in recent years. The shift in Chl phenology is also illustrated by a consistent change in the timing and onset of the spring bloom. Our analyses show that the timing of the Chl spring bloom (in month unit, all sites together) occurs significantly earlier from the 1970s to the 2010s (Fig. 7 and Table 5). This forward shift was also significant for five individual sampling sites (Table 5). The onset of the spring bloom (in month unit, all sites together) also shows a significant forward shift (Fig. 7 and Table 5). However, there is much more variability between sites, and only at Noordwijk 2 does the onset of the spring bloom show a significant forward shift (Table 5).

A change in spring bloom phenology is also shown in Fig. 8 where the $Chl^{March}_{standardized}$ shows increasing values from year to year, especially after 2000. In contrast, the $Chl^{May}_{standardized}$ tends
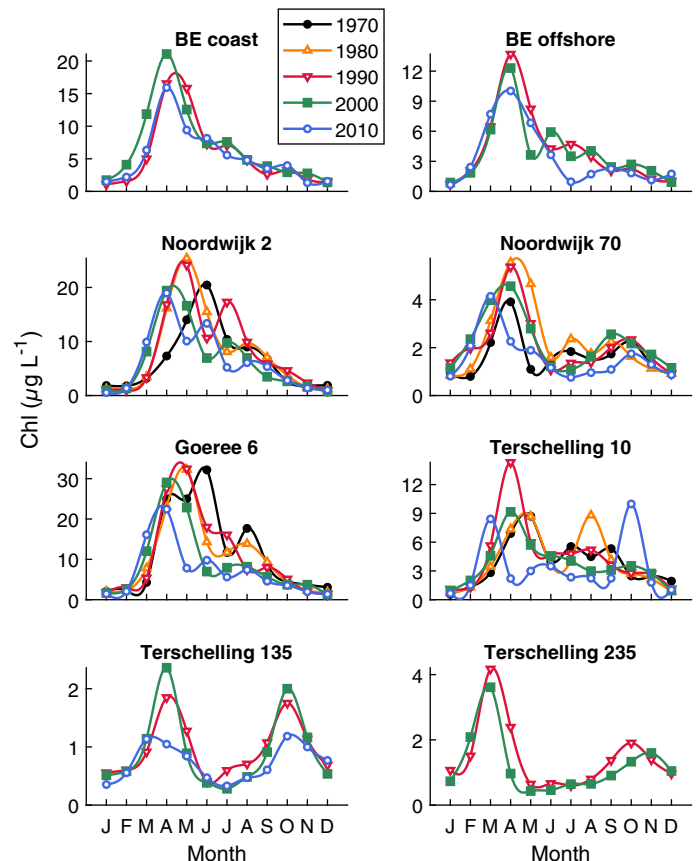
Fig. 6. Seasonal profile of Chl per decade for a selection of sampling sites in the North Sea. The lines are interpolating splines on the monthly-averaged values. The waterbodies "BE coastal" and "BE offshore" result from the aggregation of corresponding sampling sites (*see* Table 2).
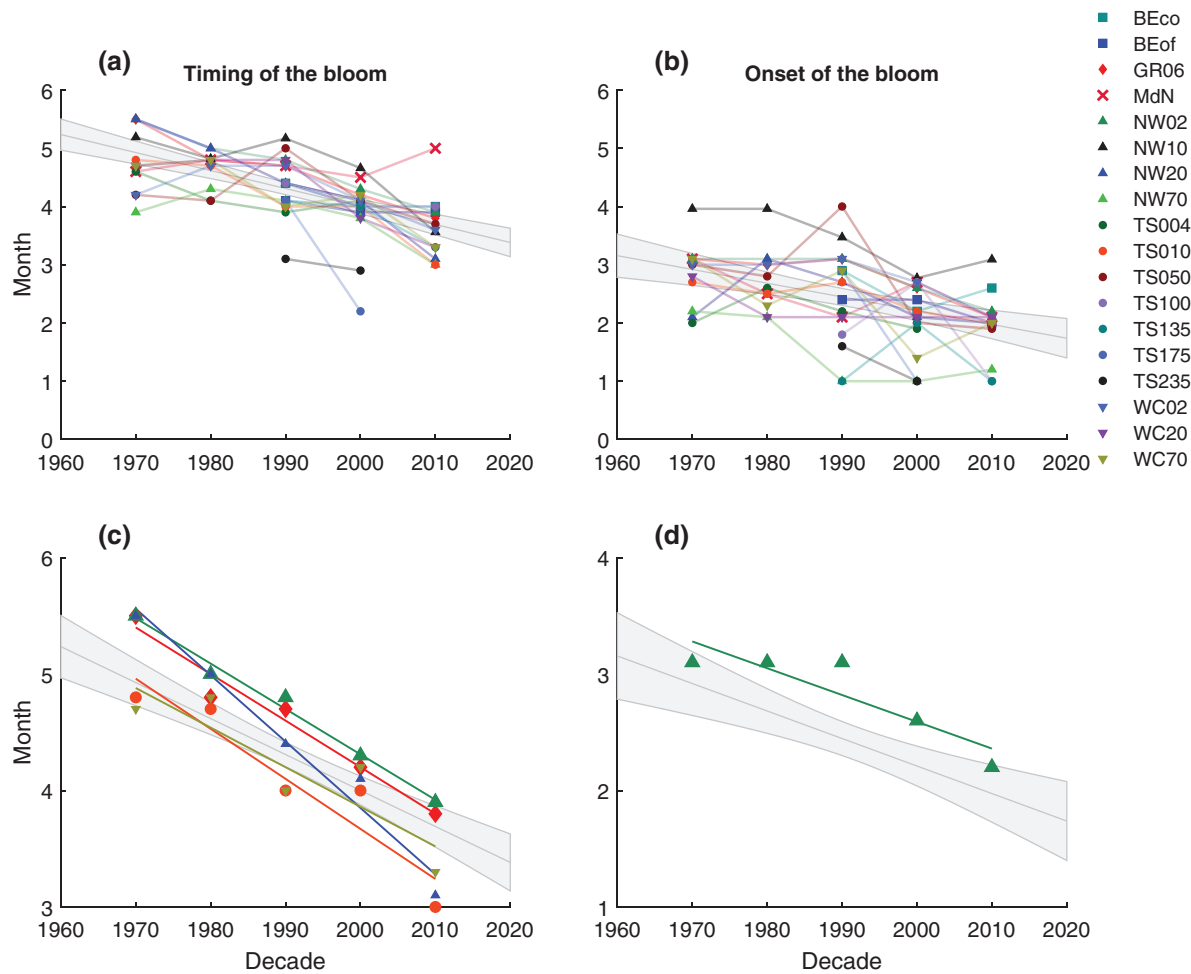
Fig. 7. Decadal change in the timing (**a**) and onset (**b**) of the Chl spring bloom at the sampling sites. (**c**) and (**d**) show the same data as (a) and (b), respectively, but only for sampling sites with a statistically significant regression line (straight lines; see statistics in Table 5). The gray regression line in the background and its confidence interval curves (95%) correspond to the regression made from all eighteen sampling sites together.

to decrease after 2000. A Pettitt's test on both time series reveals a change in central tendency in the year 2000. This further supports our previous results showing an ongoing forward shift in the Chl spring bloom.

Linear correlations investigating possible relationships between annual mean Chl and winter nutrients or SST did not show significant results, except at Marsdiep Noord ("Chl

vs. winter DIN": slope = 0.081, $R^2 = 0.30$, $p = 0.001$; and "Chl vs. winter DIP": slope = 2.05, $R^2 = 0.45$, $p < 0.001$) and at Ter-schelling 4 ("Chl vs. SST": slope = -0.969, $R^2 = 0.21$, $p = 0.031$). We also did not find a significant correlation between $Chl^{March}_{standardized}$ or $Chl^{May}_{standardized}$ and SST_{NS} over the years.

A pH time series of the Belgian data set (aggregated across the BCS) is shown in Fig. 9; an analysis for the DCS can be

Table 5. Statistics of the regression lines for the decadal evolution of the timing and onset of the Chl spring bloom in sampling sites where significant. "All sites" corresponds to the regression line made from all sampling sites together.

	Timing						Onset	
	All sites	GR06	NW02	NW20	TS010	WC70	All sites	NW02
Slope	−3.09E-02	−4.00E-02	−3.90E-02	−5.70E-02	−4.30E-02	−3.40E-02	−2.36E-02	−2.30E-02
Intercept	65.77	84.20	82.31	117.9	89.67	71.86	49.46	48.59
R^2	0.46	0.95	0.98	0.96	0.85	0.72	0.20	0.72
p value	2.1E-11	2.9E-03	6.0E-04	2.2E-03	1.6E-02	4.3E-02	4.1E-05	4.3E-02
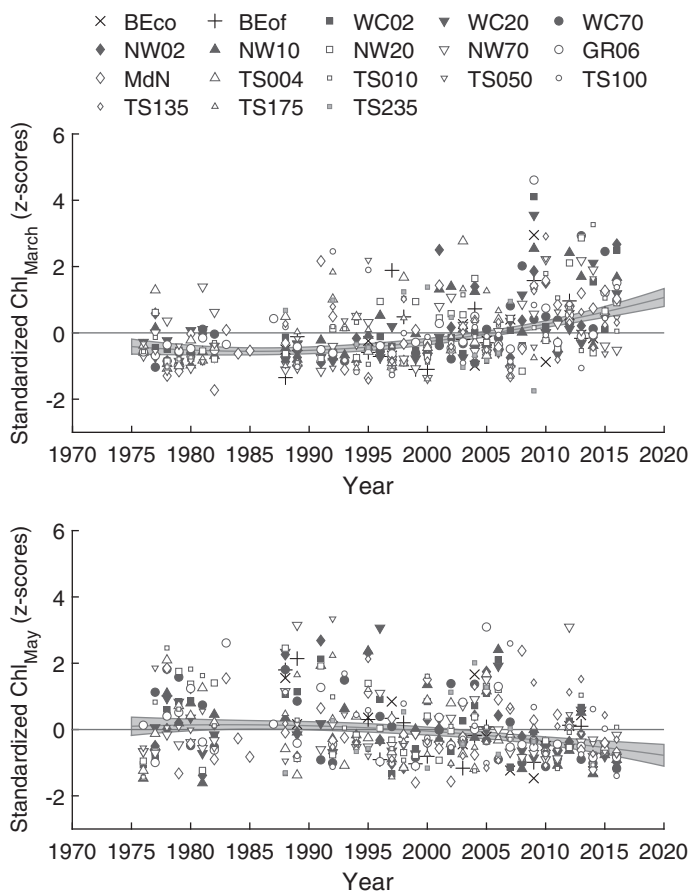
Fig. 8. (Top) Standardized Chl values in March for each year in the period 1975–2016 at all sampling sites. The quadratic regression curve is shown with its confidence intervals (ci: 95%; $R^2 = 0.22$; p value 1st parameter = 1.2×10^{-6}; p value 2nd parameter = 1.3×10^{-6}). (Bottom) Standardized Chl values in May for each year in the period 1975–2016 at all sampling sites. The quadratic regression curve is shown with its confidence intervals (ci: 95%; $R^2 = 0.06$; p value 1st parameter = 4.0×10^{-2}; p value 2nd parameter = 4.1×10^{-2}).
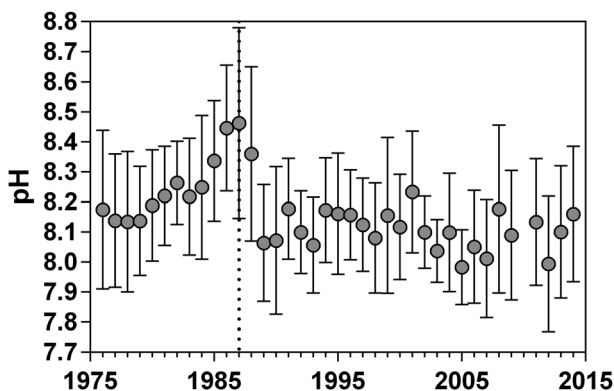
Fig. 9. Time series of pH in the Belgian continental shelf (Southern North Sea) over the period 1975–2015. Gray dots are arithmetic averages and their associated vertical lines are ± SDs.

found in Provoost et al. (2010). Annual means of pH in the BCS show a gradual increase from the early 1970s to the mid-1980s, followed by a sharp decrease around 1989, after which the values more or less stabilize (Fig. 9).

This trend is also visible in the seasonal amplitude of pH (calculated as the difference between the monthly minimum and maximum for a given year; Fig. 10). During the period 1975–2015, the seasonal signal of pH also showed a change during the phytoplankton bloom with high values shifting from late to early spring. This is apparent in the detrended signal of pH in April and May (Fig. 10): while the pH anomaly increases in April, it globally decreases in May (starting from the 1980s).

Discussion

At least two major drivers of phytoplankton production have changed in recent decades in the North Sea: SST has increased by 1.6°C between 1971 and 2014, and the N and P loads from surrounding rivers have decreased from the mid-1980s onward. There is still debate about the causal factors of the North Sea warming trend. Some authors attribute it mainly to an increase in Northern Hemisphere Temperature (e.g., Beaugrand and Reid 2003), while van Aken (2010) also points out the contribution of local variations in wind circulation and cloudiness, not excluding the influence of the climate warming due to greenhouse gases.

In the same period, the marine winter DIN and DIP concentrations decreased at most sampling sites under freshwater influence, following the N and P load reduction in rivers surrounding the North Sea. The four most important anthropogenic sources of N and P are the rivers Rhine, Humber, Seine, and Elbe, together accounting for 56% and 63%, respectively, of the N and P loads from the rivers listed in Table 1. Atmospheric N deposition to the sea is not a negligible anthropogenic source in the Southern Bight (especially in offshore areas), with relative contributions between 10% and 30% (Dulière et al. 2017). The high values of N and P found in the 1980s in both rivers and marine sampling sites are in line with the maximum N and P concentrations found during the 1980s in long time series of the River Rhine going back to the 19th century (van Beusekom 2018). The decline in P inputs to the rivers since the late 1980s reflects improved waste water treatments and limits on the phosphorus content of laundry detergents (EC 2010; Bouraoui et al. 2014). The reduction of N inputs to the rivers has been less pronounced, mainly due to the difficulty in controlling diffuse agricultural sources. Typically, the response time before the impact of an N reduction is seen in surface waters may amount to several decades because of N storage in soils and aquifers (Bouraoui and Grizzetti 2011). The reductions had an impact on coastal concentrations of nutrients, with a statistically significant decrease in winter DIN and DIP at 9 and 11 out of 18 sites, respectively (Fig. 4 and Table 3). The marine offshore sites did not exhibit
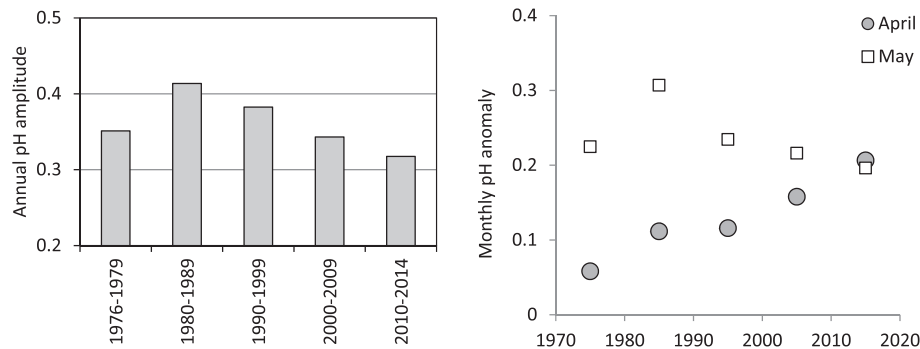
Fig. 10. (Left) Annual pH amplitude (calculated as the difference between the monthly maximum and minimum per yearly cycle) per decade in the BCS. (Right) Monthly anomalies of pH in April and May in the BCS.

trends in nutrient concentration as they are mainly under the influence of Atlantic waters (Dulière et al. 2017; Lenhart and Große 2018; Ménesguen et al. 2018). BE offshore is an exception as it shows a decreasing trend in winter DIP. Although that waterbody is dominated by Channel waters, it is also under the influence of the Scheldt and the remnant of the buoyant plumes from the Seine and Somme rivers (Ménesguen et al. 2018). The dissolved silica (DSi) loads are lower than the N loads in most rivers, resulting in on average high N:Si ratios at the river outlets. According to Prins et al. (2012), the export of silica to the coastal zone has increased in some areas since the 1990s due to lower riverine diatom production resulting from de-eutrophication. This may potentially stimulate marine diatom production.

A decline in the annual mean Chl since the 1990s was observed at eleven out of eighteen sampling sites, mostly in coastal waters subject to freshwater influence. At the same time, an overall change in Chl phenology was also observed, with the onset and timing of the spring bloom occurring earlier in the year. These observations are consistent with the long-term pH trend, which shows an increase until 1988, followed by a decline, and changes in the monthly pH signal which corroborate the observed forward shift of the Chl spring bloom. Indeed, pH increases when net phytoplankton photosynthesis increases and organic matter accumulates, and the annual amplitude of the pH signal can be interpreted as a proxy of the net annual phytoplankton production (Borges and Frankignoulle 1999). The long-term trend in pH and its annual amplitude may therefore be related to changes in phytoplankton production, possibly in response to the eutrophication and de-eutrophication processes before and after the late 1980s (Lancelot et al. 2007; Borges and Gypens 2010). Our observations are in general agreement with known North Sea ecosystem regime shifts (around 1979, 1988, and perhaps 1998) with changes in the abundance and diversity of planktonic species (Beaugrand and Reid 2003; Edwards et al. 2006, for 1988 and Alvarez-Fernandez et al. 2012; Weijerman et al. 2005, for 1998). According to Weijerman et al. (2005), the regime shift of 1988 is linked to changes in SST and weather conditions, with an increased inflow of relatively warm Atlantic water. Our results support the regime shift of 1988 and the potential regime shift of 1998. The long-term increase in SST_{NS} is marked by two tipping points: 1987–1988 and 1996–1998. Furthermore, the annual mean Chl at 12 sites also show tipping points in the period 1995–2007, while the change in Chl phenology is also marked by a tipping point in the year 2000 (i.e., increasing $Chl^{March}_{standardized}$ and decreasing $Chl^{May}_{standardized}$ across all sampling sites).

Many studies have reported long-term changes in phytoplankton biomass proxies (including Chl but also the Phytoplankton Colour Index obtained with the CPR, McQuatters-Gollop et al. 2015) in the North Sea. In general, phytoplankton biomass appears to have increased from the 1970s to 1990s/2000s (Philippart et al. 2000; Beaugrand and Reid 2003; Antoine et al. 2005; Edwards et al. 2006; McQuatters-Gollop et al. 2007; Raitsos et al. 2014). However, several studies showed a stabilization or decline in phytoplankton biomass and/or production after the late 1990s (Cadée and Hegeman 2002; Prins et al. 2012; Capuzzo et al. 2015, 2018), which is in accordance with our observations. These changes in phytoplankton biomass could either be directly linked to changes in important drivers of phytoplankton production, such as temperature, nutrients, or the underwater light climate, or indirectly, via the effect of these drivers on, for example, changes in stratification regimes or zooplankton/benthos grazing (Cloern 2001). The fact that we did not observe a direct significant correlation between the annual or seasonal dynamics of Chl and nutrients or temperature suggests that complex interactions between the abovementioned factors may underlie the Chl trends.

Several studies reported that a reduction in riverine nutrient loads will impact coastal phytoplankton production through nutrient limitation (Rousseau et al. 2006; Lacroix et al. 2007; Lenhart et al. 2010; Desmit et al. 2015). The observed decline in Chl in the present study can also be linked with reduced riverine nutrient inputs since the late 1980s. However, offshore waterbodies like BE offshore, Walcheren

70, Noordwijk 70, and Terschelling 100 also exhibit a declining trend in annual mean Chl (and Terschelling 135 shows a change in central tendency toward lower values over the period) but do not show a significant decreasing trend in nutrient concentrations (except for P in BE offshore, but it has been argued that N is limiting there; Burson et al. 2016; Desmit et al. 2015). Likewise, the shift in Chl phenology cannot directly result from a change in marine nutrient concentrations. At sites under freshwater influence, winter nutrient concentrations show lower values in recent decades because of de-eutrophication but their seasonal signal did not change (i.e., the minimum concentration of nutrients is reached the same month; *see* Fig. S3). Moreover, the forward shift in the timing of the spring bloom is also visible at an offshore sampling site, Walcheren 70, where nutrient concentrations are more stable (Table 3).

While increases in phytoplankton biomass until the 1990s/2000s have been attributed to climate warming (e.g., Raitsos et al. 2014), rising temperature may also have adverse effects on phytoplankton density. Barton et al. (2018) proposed a physiological mechanism to explain the possible link between rising temperatures and a decline in phytoplankton biomass. The capacity of phytoplankton to efficiently use its photosynthetic carbon to grow could be limited at higher temperatures by rising respiratory costs exceeding the supply of reduced carbon from photosynthesis (Barton et al. 2018). Another explanation for the decrease in Chl could be that the Carbon:Chl ratio of phytoplankton increases with water clarity, as observed by Alvarez-Fernandez and Riegman (2014).

The forward shift in phytoplankton bloom phenology may be linked with increased winter and early spring temperatures (*see* Beaugrand and Reid 2003; Edwards et al. 2006). A mechanistic explanation was proposed by Hunter-Cevera et al. (2016): increasing temperature accelerates phytoplankton cell division rates, resulting in earlier bloom formation. It is, however, commonly considered that the onset of the spring bloom in the North Sea depends on both temperature and light availability (Peperzak 1993; Peperzak et al. 1998). Therefore, another explanation could involve a change in the underwater light field in recent decades either through a change in cloudiness and hence surface irradiance, or through a change in turbidity. Wiltshire et al. (2008) reported an increase in water transparency at Helgoland Roads but, even so, they did not observe a change in the spring bloom dynamics. In the BCS, SPM loads were slightly but significantly lower in the 2000s compared with the 1970s, but only in winter (A. Nohe unpubl. obs.), which may result in a more favorable light climate for phytoplankton growth in late winter–early spring. In contrast, Capuzzo et al. (2015) showed that water clarity in the North Sea has generally decreased in the last decades, driven largely by increased suspended sediment, except perhaps in the permanently mixed areas of the Southern Bight including the Belgian coast. Although water clarity may have increased locally (Wiltshire et al. 2008; Alvarez-Fernandez and

Riegman 2014), it seems that the general trend in the North Sea is toward a decrease in water clarity.

Another important temperature-related factor impacting phytoplankton growth is stratification. In seasonally stratified regions, the thermal stratification cycle is set by the balance between seasonal heating and tidal mixing, with wind mixing perturbing this stratification cycle throughout the year (Holt et al. 2016). Stratification reduces the adverse effect of light limitation on phytoplankton production but may cause nutrient limitation in summer, unless stratification is interrupted. The phytoplankton bloom will then be sensitive to factors that strengthen the stratification (e.g., increasing SST) or that interrupt it (e.g., strong wind). Capuzzo et al. (2018) propose that the decline in phytoplankton production across the North Sea in recent decades may be explained by reduced nutrient inputs (particularly in the Southern Bight) and indirect effects of temperature such as a strengthening of the density gradient at the thermocline. Holt et al. (2016) pointed out increased stratification and decreased phytoplankton production in the central (stratified) parts of the North Sea. The decreasing trend in wind speed at meteorological stations on the Dutch coast suggests that the increase in stratification (strength, duration) with increased temperatures is further enhanced by changes in the wind climate. In this respect, the seasonal profiles of Chl at Terschelling 10 and at Terschelling 235 (Fig. 6) suggest a longer duration of the summer stratification in recent years shifting the autumn Chl bloom to October and November, respectively.

Zooplankton grazing may have significant control over phytoplankton dynamics and the bloom formation in the North Atlantic (Behrenfeld 2010). Following the "dilution-recoupling hypothesis," cold winters and associated deep mixing are essential for the bloom formation in seasonally stratified areas. Deep mixing perturbs predator-prey interactions through dilution effect and allows the net growth rate of phytoplankton to be positive in mid-winter or early spring. The phytoplankton annual cycle and community structure may also change dramatically under shifting grazing pressure, as shown in the San Francisco Bay when the Pacific Ocean shifted from its warm phase to its cold phase in 1999 (Cloern et al. 2007; Smetacek and Cloern 2008). In the North Sea, the warm regime since the late 1980s was accompanied by a decrease of cold-water copepods and an increase of warm-water copepods (CPR data; Alvarez-Fernandez et al. 2012). The authors also observed a decrease in dinoflagellates and an increase in diatoms annual maxima after 1998. In mesocosm experiments, Keller et al. (1999) showed that warmer temperatures result in lower phytoplankton biomass during the winter-spring bloom period. This may be attributed to increase grazing related to greater metabolic activity of zooplankton and benthos. In the shallow List Tidal Basin (Wadden Sea), van Beusekom et al. (2009) showed a negative correlation between spring Chl (mean March–April) and winter temperature (mean February–March). Cold winters are followed by

higher Chl spring blooms; the potential reason being that "phytoplankton loss by benthic filtration and/or zooplankton grazing is reduced by low temperatures thereby enhancing the bloom magnitude" (van Beusekom et al. 2009). These results tend to suggest that, in shallow or seasonally stratified areas, a warming trend may result in less intense spring bloom due to enhanced grazing/filtration. Top-down control in the North Sea was, however, questioned by Capuzzo et al. (2018) who provided evidence for a bottom-up effect of decreasing phytoplankton production on higher trophic levels. The decline in annual mean Chl and the shift in phytoplankton phenology may indeed have an impact on the food web. The trophic "match-mismatch" hypothesis (Cushing 1990) predicts that after a phenological shift a predator may miss the production peak of its prey as the level of response to drivers of change (e.g., climate warming) may vary across functional groups and multiple trophic levels (Edwards and Richardson 2004). This effect may be reduced in temperate productive systems, however, as pointed out by Atkinson et al. (2015): the variability in relative timing of feeder and food is naturally high in the marine system and, thus, some compensating mechanisms exist to reduce the impact of a planktonic phenological shift on the trophic transfers, potentially reducing adverse effects.

To summarize, the sea surface warming and the de-eutrophication trend since the mid-1980s in the North Sea may have directly affected phytoplankton photosynthesis in the North Sea, but also indirectly via changes in stratification or grazing. The combination of these factors may have induced a decline in annual mean Chl and a forward shift in the spring bloom of Chl across the North Sea, with a tipping point around 2000. However, the exact mechanisms for the observed Chl changes remain as yet unclear, and it would be interesting to further compare the North Sea with other temperate marine areas subject to de-eutrophication and warming.

References

Alvarez-Fernandez, S., H. Lindeboom, and E. Meesters. 2012. Temporal changes in plankton of the North Sea: Community shifts and environmental drivers. Mar. Ecol. Prog. Ser. **462**: 21–38. doi:10.3354/meps09817

Alvarez-Fernandez, S., and R. Riegman. 2014. Chlorophyll in North Sea coastal and offshore waters does not reflect long term trends of phytoplankton biomass. J. Sea Res. **91**: 35–44. doi:10.1016/J.SEARES.2014.04.005

Antoine, D., A. Morel, H. Gordon, V. Banzon, and R. Evans. 2005. Bridging ocean color observations of the 1980s and 2000s in search of long-term trends. J. Geophys. Res. **110**: C002620. doi:10.1029/2004JC002620

Atkinson, A., R. A. Harmer, C. E. Widdicombe, A. J. McEvoy, T. J. Smyth, D. G. Cummings, P. J. Somerfield, J. L. Maud, and K. McConville. 2015. Questioning the role of phenology shifts and trophic mismatching in a planktonic food

web. Prog. Oceanogr. **137**: 498–512. doi:10.1016/J.POCEAN.2015.04.023

Barton, S., J. Jenkins, A. Buckling, C.-E. Schaum, N. Smirnoff, and G. Yvon-Durocher. 2018. Universal metabolic constraints on the thermal tolerance of marine phytoplankton. bioRxiv: 358002. doi:10.1101/358002

Beamish, R. J., D. J. Noakes, G. A. McFarlane, L. Klyashtorin, V. V. Ivanov, and V. Kurashov. 1999. The regime concept and natural trends in the production of Pacific salmon. Can. J. Fish. Aquat. Sci. **56**: 516–526. doi:10.1139/f98-200

Beaugrand, G., and P. C. Reid. 2003. Long-term changes in phytoplankton, zooplankton and salmon related to climate. Glob. Chang. Biol. **9**: 801–817. doi:10.1046/j.1365-2486.2003.00632.x

Behrenfeld, M. J. 2010. Abandoning Sverdrup's critical depth hypothesis on phytoplankton blooms. Ecology **91**: 977–989. doi:10.1890/09-1207.1

Billen, G., and others. 2011. Nitrogen flows from European watersheds to coastal marine waters, p. 271–297. *In* The European nitrogen assessment: Sources, effects, and policy perspectives. Cambridge Univ. Press.

Borges, A., and M. Frankignoulle. 1999. Daily and seasonal variations of the partial pressure of CO_2 in surface seawater along Belgian and southern Dutch coastal areas. J. Mar. Syst. **19**: 251–266. doi:10.1016/S0924-7963(98)00093-1

Borges, A. V., and N. Gypens. 2010. Carbonate chemistry in the coastal zone responds more strongly to eutrophication than ocean acidification. Limnol. Oceanogr. **55**: 346–353. doi:10.4319/lo.2010.55.1.0346

Bouraoui, F., and B. Grizzetti. 2011. Long term change of nutrient concentrations of rivers discharging in European seas. Sci. Total Environ. **409**: 4899–4916. doi:10.1016/J.SCITOTENV.2011.08.015

Bouraoui, F., V. Thieu, B. Grizzetti, W. Britz, and G. Bidoglio. 2014. Scenario analysis for nutrient emission reduction in the European inland waters. Environ. Res. Lett. **9**: 1–13. doi:10.1088/1748-9326/9/12/125007

Brion, N., S. Jans, L. Chou, and V. Rousseau. 2006. Nutrient loads to the Belgian Coastal Zone, p. 17–43. *In* V. Rousseau, C. Lancelot, and D. Cox [eds.], Current status of eutrophication in the Belgian coastal zone. Brussels: Presses Univ. de Bruxelles.

Burson, A., M. Stomp, L. Akil, C. P. D. Brussaard, and J. Huisman. 2016. Unbalanced reduction of nutrient loads has created an offshore gradient from phosphorus to nitrogen limitation in the North Sea. Limnol. Oceanogr. **61**: 869–888. doi:10.1002/lno.10257

Cadée, G. C., and J. Hegeman. 2002. Phytoplankton in the Marsdiep at the end of the 20th century; 30 years monitoring biomass, primary production, and Phaeocystis blooms. J. Sea Res. **48**: 97–110. doi:10.1016/S1385-1101(02)00161-2

Capuzzo, E., and others. 2018. A decline in primary production in the North Sea over 25 years, associated with reductions in zooplankton abundance and fish stock

recruitment. Glob. Chang. Biol. **24**: e352–e364. doi:10.1111/gcb.13916

Capuzzo, E., D. Stephens, T. Silva, J. Barry, and R. M. Forster. 2015. Decrease in water clarity of the southern and central North Sea during the 20th century. Glob. Chang. Biol. **21**: 2206–2214. doi:10.1111/gcb.12854

Cloern, J. E. 2001. Our evolving conceptual model of the coastal eutrophication problem. Mar. Ecol. Prog. Ser. **210**: 223–253. doi:10.3354/meps210223

Cloern, J. E., and A. D. Jassby. 2010. Patterns and scales of phytoplankton variability in estuarine–coastal ecosystems. Estuar. Coast. **33**: 230–241. doi:10.1007/s12237-009-9195-3

Cloern, J. E., A. D. Jassby, J. K. Thompson, and K. A. Hieb. 2007. A cold phase of the East Pacific triggers new phytoplankton blooms in San Francisco Bay. Proc. Natl. Acad. Sci. USA **104**: 18561–18565. doi:10.1073/pnas.0706151104

Colijn, F., K.-J. Hesse, N. Ladwig, and U. Tillmann. 2002. Effects of the large-scale uncontrolled fertilisation process along the continental coastal North Sea, p. 133–148. *In* Sustainable increase of marine harvesting: Fundamental mechanisms and new concepts. Dordrecht, the Netherlands: Springer. doi:10.1007/978-94-017-3190-4_12

Conley, D., H. Paerl, R. Howarth, D. Boesch, S. Seitzinger, K. Havens, C. Lancelot, and G. Likens. 2009. Controlling eutrophication: nitrogen and phosphorus. Science **323**: 1014–1015.

Cushing, D. H. 1990. Plankton production and year-class strength in fish populations: An update of the match/mismatch hypothesis. Adv. Mar. Biol. **26**: 249–293. doi:10.1016/S0065-2881(08)60202-3

Daro, M.-H., E. Breton, E. Antajan, S. Gasparini, and V. Rousseau. 2006. Do Phaeocystis colony blooms affect zooplankton in the Belgian coastal zone? p. 61–72. *In* V. Rousseau, C. Lancelot, and D. Cox [eds.], Current status of eutrophication in the Belgian coastal zone. Brussels: Presses Univ. de Bruxelles.

de Boer, G. J., J. D. Pietrzak, and J. C. Winterwerp. 2009. SST observations of upwelling induced by tidal straining in the Rhine ROFI. Cont. Shelf Res. **29**: 263–277. doi:10.1016/J.CSR.2007.06.011

De Galan, S., M. Elskens, L. Goeyens, A. Pollentier, N. Brion, and W. Baeyens. 2004. Spatial and temporal trends in nutrient concentrations in the Belgian Continental area of the North Sea during the period 1993–2000. Estuar. Coast. Shelf Sci. **61**: 517–528. doi:10.1016/J.ECSS.2004.06.015

de Jong, F. 2007. Marine eutrophication in perspective: On the relevance of ecology for environmental policy. Springer Science & Business Media.

de Jonge, V. N., M. Elliott, and E. Orive. 2002. Causes, historical development, effects and future challenges of a common environmental problem: eutrophication, p. 1–19. *In* Nutrients and eutrophication in estuaries and coastal waters. Dordrecht, the Netherlands: Springer. doi:10.1007/978-94-017-2464-7_1

Desmit, X., K. Ruddick, and G. Lacroix. 2015. Salinity predicts the distribution of chlorophyll a spring peak in the southern North Sea continental waters. J. Sea Res. **103**: 59–74. doi:10.1016/j.seares.2015.02.007

Desmit, X., and others. 2018. Reducing marine eutrophication may require a paradigmatic change. Sci. Total Environ. **635**: 1444–1466. doi:10.1016/j.scitotenv.2018.04.181

Diaz, R. J., and R. Rosenberg. 2008. Spreading dead zones and consequences for marine ecosystems. Science **321**: 926–929. doi:10.1126/science.1156401

Directive_2000/60/EC. 2000. Directive 2000/60/EC of the European Parliament and of the Council of 23 October 2000 establishing a framework for Community action in the field of water policy. Official Journal of the European Communities 327/1.

Directive_2008/56/EC. 2008. Directive 2008/56/EC of the European Parliament and of the Council of 17 June 2008 establishing a framework for community action in the field of marine environmental policy (Marine Strategy Framework Directive). Official Journal of the European Union 164/19.

Directive_91/271/EEC. 1991. Council Directive concerning urban waste water treatment (91/271/EEC). Off. J. 135.

Directive_91/676/EEC. 1991. Council Directive concerning the protection of waters against pollution caused by nitrates from agricultural sources (91/676/EEC). Off. J. 375.

Doney, S. C. 2010. The growing human footprint on coastal and open-ocean biogeochemistry. Science **328**: 1512–1516. doi:10.1126/science.1185198

Dulière, V., N. Gypens, C. Lancelot, P. Luyten, and G. Lacroix. 2017. Origin of nitrogen in the English Channel and Southern Bight of the North Sea ecosystems. Hydrobiologia: 1–21. doi:10.1007/s10750-017-3419-5

EC. 2010. Commission Proposal amending Regulation (EC) No 648/2004 as regards the use of phosphates and other phosphorus compounds in household laundry detergents.

Edwards, M., D. G. Johns, S. C. Leterme, E. Svendsen, and A. J. Richardson. 2006. Regional climate change and harmful algal blooms in the northeast Atlantic. Limnol. Oceanogr. **51**: 820–829. doi:10.4319/lo.2006.51.2.0820

Edwards, M., and A. J. Richardson. 2004. Impact of climate change on marine pelagic phenology and trophic mismatch. Nature **430**: 881–884. doi:10.1038/nature02808

Galloway, J. N., and others. 2004. Nitrogen cycles: Past, present, and future. Biogeochemistry **70**: 153–226. doi:10.1007/s10533-004-0370-0

Grasshoff, K., M. Ehrhardt, and K. Kremling. 1983. Methods of seawater analysis. Weinheim, Germany: Verlag Chemie.

Holt, J., and others. 2016. Potential impacts of climate change on the primary production of regional seas: A comparative analysis of five European seas. Prog. Oceanogr. **140**: 91–115. doi:10.1016/J.POCEAN.2015.11.004

Howarth, R. W., and R. Marino. 2006. Nitrogen as the limiting nutrient for eutrophication in coastal marine ecosystems:

Evolving views over three decades. Limnol. Oceanogr. **51**: 364–376. doi:10.4319/lo.2006.51.1_part_2.0364

Høyer, J. L., and I. Karagali. 2016. Sea surface temperature climate data record for the North Sea and Baltic Sea. J. Clim. **29**: 2529–2541. doi:10.1175/JCLI-D-15-0663.1

Hunter-Cevera, K. R., M. G. Neubert, R. J. Olson, A. R. Solow, A. Shalapyonok, and H. M. Sosik. 2016. Physiological and ecological drivers of early spring blooms of a coastal phytoplankter. Science **354**: 326–329. doi:10.1126/science.aaf8536

Jickells, T. D. 1998. Nutrient biogeochemistry of the coastal zone. Science **281**: 217–221. doi:10.1126/SCIENCE.281.5374.217

Keller, A. A., C. A. Oviatt, H. A. Walker, and J. D. Hawk. 1999. Predicted impacts of elevated temperature on the magnitude of the winter-spring phytoplankton bloom in temperate coastal waters: A mesocosm study. Limnol. Oceanogr. **44**: 344–356. doi:10.4319/lo.1999.44.2.0344

Koroleff, F. 1969. Direct determination of ammonia in natural waters as indophenol blue. International Council for Exploration of the Sea. 19–22.

Lacroix, G., K. Ruddick, N. Gypens, and C. Lancelot. 2007. Modelling the relative impact of rivers (Scheldt/Rhine/Seine) and Western Channel waters on the nutrient and diatoms/Phaeocystis distributions in Belgian waters (Southern North Sea). Cont. Shelf Res. **27**: 1422–1446. doi:10.1016/j.csr.2007.01.013

Lagring, R., and others. 2018. 4 Decades of Belgian Marine Monitoring: Uplifting historical data to today's needs— Final Report. Brussels.

Lancelot, C., G. Billen, A. Sournia, T. Weisse, F. Colijn, M. J. W. Veldhuis, A. Davies, and P. Wassman. 1987. Phaeocystis blooms and nutrient enrichment in the continental coastal zones of the North Sea. Ambio **16**: 38–46. doi:10.2307/4313316

Lancelot, C., N. Gypens, G. Billen, J. Garnier, and V. Roubeix. 2007. Testing an integrated river-ocean mathematical tool for linking marine eutrophication to land use: The Phaeocystis-dominated Belgian coastal zone (Southern North Sea) over the past 50 years. J. Mar. Syst. **64**: 216–228. doi:10.1016/j.jmarsys.2006.03.010

Lancelot, C., P. Passy, and N. Gypens. 2014. Model assessment of present-day Phaeocystis colony blooms in the Southern Bight of the North Sea (SBNS) by comparison with a reconstructed pristine situation. Harmful Algae **37**: 172–182. doi:10.1016/j.hal.2014.05.017

Lenhart, H.-J., and F. Große. 2018. Assessing the effects of WFD nutrient reductions within an OSPAR frame using trans-boundary nutrient modeling. Front. Mar. Sci. **5**: 447. doi:10.3389/fmars.2018.00447

Lenhart, H. J., and others. 2010. Predicting the consequences of nutrient reduction on the eutrophication status of the North Sea. J. Mar. Syst. **81**: 148–170. doi:10.1016/j.jmarsys.2009.12.014

Longhurst, A. 2007. Ecological geography of the sea, 2nd ed. Elsevier Inc.

MATLAB. 2018. version 9.4.0.813654 (R2018a). Natick, Massachusetts: The MathWorks Inc.

McQuatters-Gollop, A., M. Edwards, P. Helaouët, D. G. Johns, N. J. P. Owens, D. E. Raitsos, D. Schroeder, J. Skinner, and R. F. Stern. 2015. The Continuous Plankton Recorder survey: How can long-term phytoplankton datasets contribute to the assessment of Good Environmental Status? Estuar. Coast. Shelf Sci. **162**: 88–97. doi:10.1016/J.ECSS.2015.05.010

McQuatters-Gollop, A., D. E. Raitsos, M. Edwards, Y. Pradhan, L. D. Mee, S. J. Lavender, and M. J. Attrill. 2007. A long-term chlorophyll dataset reveals regime shift in North Sea phytoplankton biomass unconnected to nutrient levels. Limnol. Oceanogr. **52**: 635–648. doi:10.4319/lo.2007.52.2.0635

Ménesguen, A., X. Desmit, V. Dulière, G. Lacroix, B. Thouvenin, V. Thieu, and M. Dussauze. 2018. How to avoid eutrophication in coastal seas? A new approach to derive river-specific combined nitrate and phosphate maximum concentrations. Sci. Total Environ. **628–629**: 400–414. doi:10.1016/j.scitotenv.2018.02.025

Meyer, J., P. Nehmer, A. Moll, and I. Kröncke. 2018. Shifting south-eastern North Sea macrofauna community structure since 1986: A response to de-eutrophication and regionally decreasing food supply? Estuar. Coast. Shelf Sci. **213**: 115–127. doi:10.1016/J.ECSS.2018.08.010

Mieruch, S., J. A. Freund, U. Feudel, M. Boersma, S. Janisch, and K. H. Wiltshire. 2010. A new method of describing phytoplankton blooms: Examples from Helgoland Roads. J. Mar. Syst. **79**: 36–43. doi:10.1016/J.JMARSYS.2009.06.004

Nohe, A., and others. 2018. Data Descriptor: Marine phytoplankton community composition data from the Belgian part of the North Sea, 1968-2010. Sci. Data **5**: 180126. doi:10.1038/sdata.2018.126

NSC. 1990. Ministerial Declaration. Third International Conference on the Protection of the North Sea, The Hague, 8 March 1990. Available from https://www.ospar.org/site/assets/files/1239/3nsc-1990-hague_declaration.pdf

NSC. 1987. Ministerial Declaration. Second International Conference on the Protection of the North Sea, London, 24–25 November 1987. Available from https://www.ospar.org/site/assets/files/1239/2nsc-1987_london_declaration.pdf

OSPAR_Commission. 2017. Third Integrated Report on the Eutrophication Status of the OSPAR Maritime Area.

Painting, S., and others. 2013. Impacts of climate change on nutrient enrichment. MCCIP Sci. Rev. 219–235. doi:10.14465/2013.arc23.219-235

Pätsch, J., H.-J. Lenhart, and M. Schütt. 2016. Daily loads of nutrients, total alkalinity, dissolved inorganic carbon and dissolved organic carbon of the European Continental Rivers for the Years 1977–2014. Hamburg.

Peperzak, L. 1993. Daily irradiance governs growth rate and colony formation of Phaeocystis (Prymnesiophyceae). J. Plankton Res. **15**: 809–821. doi:10.1093/plankt/15.7.809

Peperzak, L., F. Colijn, W. W. C. Gieskes, and J. C. H. Peeters. 1998. Development of the diatom-Phaeocystis spring bloom in the Dutch coastal zone of the North Sea: The silicon depletion versus the daily irradiance threshold hypothesis. J. Plankton Res. **20**: 517–537. doi:10.1093/plankt/20.3.517

Pettitt, A. N. 1979. A non-parametric approach to the change-point problem. Appl. Stat. **28**: 126. doi:10.2307/2346729

Philippart, C., G. Cadée, W. van Raaphorst, and R. Riegman. 2000. Long-term phytoplankton-nutrient interactions in a shallow coastal sea: Algal community structure, nutrient budgets, and denitrification potential. Limnol. Oceanogr. **45**: 131–144.

Philippart, C. J. M., J. J. Beukema, G. C. Cadée, R. Dekker, P. W. Goedhart, J. M. van Iperen, M. F. Leopold, and P. M. J. Herman. 2007. Impacts of nutrient reduction on coastal communities. Ecosystems **10**: 96–119. doi:10.1007/s10021-006-9006-7

Philippart, C. J. M., J. M. van Iperen, G. C. Cadée, and A. F. Zuur. 2010. Long-term field observations on seasonality in chlorophyll-a concentrations in a shallow coastal marine ecosystem, the Wadden Sea. Estuar. Coast. **33**: 286–294. doi:10.1007/s12237-009-9236-y

Pohlert, T. 2016. Non-parametric trend tests and change-point detection. R package version 0.2.0. Available from http://CRAN.R-project.org/package=trend

Prins, T. C., X. Desmit, and J. G. Baretta-Bekker. 2012. Phytoplankton composition in Dutch coastal waters responds to changes in riverine nutrient loads. J. Sea Res. **73**: 49–62. doi:10.1016/j.seares.2012.06.009

Provoost, P., S. Van Heuven, K. Soetaert, R. W. P. M. Laane, and J. J. Middelburg. 2010. Seasonal and long-term changes in pH in the Dutch coastal zone. Biogeosciences **7**: 3869–3878. doi:10.5194/bg-7-3869-2010

R Core Team. 2015. R: A language and environment for statistical computing. R Foundation for Statistical Computing, Vienna, Austria. Available from https://www.R-project.org/

Raitsos, D. E., Y. Pradhan, S. J. Lavender, I. Hoteit, A. McQuatters-Gollop, P. C. Reid, and A. J. Richardson. 2014. From silk to satellite: Half a century of ocean colour anomalies in the Northeast Atlantic. Glob. Chang. Biol. **20**: 2117–2123. doi:10.1111/gcb.12457

Ramos, M. R., and C. Cordeiro. 2013. Trend tests in time series with missing values: A case study with imputation, p. 1909–1912. *In* AIP Conference Proceedings. AIP Publishing. doi:10.1063/1.4825905

Richardson, A. J. 2008. In hot water: Zooplankton and climate change. ICES J. Mar. Sci. **65**: 279–295. doi:10.1093/icesjms/fsn028

Richardson, A. J., and D. S. Schoeman. 2004. Climate impact on plankton ecosystems in the Northeast Atlantic. Science **305**: 1609–1612. doi:10.1126/science.1100958

Rijkswaterstaat. 2009. Analyseboek monitoring zout versie 1 juni 2009. Available from http://docplayer.nl/15055365-Analyseboek-laboratoria.html

Rousseau, V., S. Becquevort, J.-Y. Parent, S. Gasparini, M.-H. Daro, M. Tackx, and C. Lancelot. 2000. Trophic efficiency of the planktonic food web in a coastal ecosystem dominated by Phaeocystis colonies. J. Sea Res. **43**: 357–372. doi:10.1016/S1385-1101(00)00018-6

Rousseau, V., Y. Park, K. Ruddick, W. Vyverman, J.-Y. Parent, and C. Lancelot. 2006. Phytoplankton blooms in response to nutrient enrichment, p. 45–59. *In* V. Rousseau, C. Lancelot, and D. Cox [eds.], Current status of eutrophication in the Belgian coastal zone. Brussels: Presses Univ. de Bruxelles.

Ruddick, K., and G. Lacroix. 2006. Hydrodynamics and meteorology of the Belgian coastal zone, p. 1–15. *In* V. Rousseau, C. Lancelot, and D. Cox [eds.], Current status of eutrophication in the Belgian coastal zone. Brussels: Presses Univ. de Bruxelles.

Smetacek, V., and J. E. Cloern. 2008. On phytoplankton trends. Science **319**: 1346–1348. doi:10.1126/science.1151330

Troost, T. A., M. Blaas, and F. J. Los. 2013. The role of atmospheric deposition in the eutrophication of the North Sea: A model analysis. J. Mar. Syst. **125**: 101–112. doi:10.1016/J.JMARSYS.2012.10.005

van Aken, H. M. 2010. Meteorological forcing of long-term temperature variations of the Dutch coastal waters. J. Sea Res. **63**: 143–151. doi:10.1016/J.SEARES.2009.11.005

van Bennekom, A. J., and F. J. Wetsteijn. 1990. The winter distribution of nutrients in the Southern Bight of the North Sea (1961–1978) and in the estuaries of the scheldt and the rhine/meuse. Netherlands J. Sea Res. **25**: 75–87. doi:10.1016/0077-7579(90)90010-E

van Beusekom, J. E. E. 2018. Eutrophication, p. 429–445. *In* M. Salomon and T. Markus [eds.], Handbook on marine environment protection. Cham: Springer International Publishing. doi:10.1007/978-3-319-60156-4_22

van Beusekom, J. E. E., M. Loebl, and P. Martens. 2009. Distant riverine nutrient supply and local temperature drive the long-term phytoplankton development in a temperate coastal basin. J. Sea Res. **61**: 26–33. doi:10.1016/J.SEARES.2008.06.005

Van Der Zee, C., and L. Chou. 2005. Seasonal cycling of phosphorus in the Southern Bight of the North Sea. Biogeosciences **2**: 27–42.

van Leeuwen, S., P. Tett, D. Mills, and J. van der Molen. 2015. Stratified and nonstratified areas in the North Sea: Long-term variability and biological and policy implications. J. Geophys. Res. Ocean. **120**: 4670–4686. doi:10.1002/2014JC010485

Vermaat, J. E., A. McQuatters-Gollop, M. A. Eleveld, and A. J. Gilbert. 2008. Past, present and future nutrient loads of the North Sea: Causes and consequences. Estuar. Coast. Shelf Sci. **80**: 53–59. doi:10.1016/J.ECSS.2008.07.005

Weijerman, M., H. Lindeboom, and A. Zuur. 2005. Regime shifts in marine ecosystems of the North Sea and Wadden Sea. Mar. Ecol. Prog. Ser. **298**: 21–39. doi:10.3354/meps298021

Wiltshire, K. H., A. M. Malzahn, K. Wirtz, W. Greve, S. Janisch, P. Mangelsdorf, B. F. J. Manly, and M. Boersma. 2008. Resilience of North Sea phytoplankton spring bloom dynamics: An analysis of long-term data at Helgoland Roads. Limnol. Oceanogr. **53**: 1294–1302. doi:10.4319/lo.2008.53.4.1294

Conflict of Interest

None declared.